1-1-2015

Backarc basin and ocean island basalts in the Narooma Accretionary Complex, Australia: setting, geochemistry and tectonics

Natalie C. Stokes
University of Wollongong, ncs822@uowmail.edu.au

Chris L. Fergusson
University of Wollongong, cferguss@uow.edu.au

R Offler
University of Newcastle

Backarc basin and ocean island basalts in the Narooma Accretionary Complex, Australia: setting, geochemistry and tectonics

Abstract

The Cambrian-Ordovician Wagonga Group contains basalts at Melville Point and Barlings Beach, 20 km south of Batemans Bay, New South Wales. At Melville Point, the succession has basal altered basalts overlain by chert and interbedded siliceous mudstone of the Wagonga Group, in turn overlain by turbidites and chert of the Adaminaby Group with a latest Cambrian to earliest Ordovician age. By contrast, at Barlings Beach, basalt is associated with highly disrupted chert (tectonic mélange), various slivers of mudstone and turbidites, and turbidites of the Adaminaby Group. Immobile elements in the basalts show consistent patterns that allow the magmatic affinity and tectonic setting to be determined in spite of pervasive hydrothermal alteration and subsequent lower greenschist facies metamorphism that accompanied strong folding and multiple foliation development. The Melville Point basalts show Ti/V ratios transitional between arc and MORB and therefore may have formed in either a forearc or backarc basin setting. However, these rocks have higher Ti/V ratios, LREE, Th and Nb than found in forearc basalts and are therefore considered to have formed in a backarc basin setting. In contrast to Melville Point, most basalts at Barlings Beach have a geochemical signature distinctive of ocean island settings like those reported from elsewhere in the Wagonga Group. We believe these rocks developed in a Cambrian backarc basin setting. In the Early to Middle Ordovician, much of the ocean basin was inundated by quartzose turbidites followed by basin destruction with accretion/underplating at a Late Ordovician-early Silurian Benambran subduction zone and formation of the Narooma Accretionary Complex.

Keywords

Backarc basin basalt, Cambrian, Lachlan Orogen, ocean island basalt, Ordovician, Narooma Accretionary Complex, New South Wales, subduction

Disciplines

Medicine and Health Sciences | Social and Behavioral Sciences

Publication Details

Stokes, N., Fergusson, C. L. & Offler, R. (2015). Backarc basin and ocean island basalts in the Narooma Accretionary Complex, Australia: setting, geochemistry and tectonics. Australian Journal of Earth Sciences, 62 (1), 37-53.

Backarc basin and ocean island basalts in the Narooma Accretionary Complex, Australia: setting, geochemistry and tectonics

N. STOKES[1,2], C. L. FERGUSSON[1*] AND R. OFFLER[3]

[1]School of Earth & Environmental Sciences, University of Wollongong, NSW 2522, Australia

[2]Present address: GHD, 145 Ann St Brisbane, QLD 4000, Australia

[3]New South Wales Institute of Frontiers Geoscience, School of Environmental and Life Sciences, University of Newcastle, NSW 2308, Australia

[*]cferguss@uow.edu.au

Running Title: Basalts of the Narooma Accretionary Complex

The Cambrian–Ordovician Wagonga Group contains basalts at Melville Point and Barlings Beach, 20 km south of Batemans Bay, New South Wales. At Melville Point, the succession has basal altered basalts overlain by chert and interbedded siliceous mudstone of the Wagonga Group, in turn overlain by turbidites and chert of the Adaminaby Group with a latest Cambrian to earliest Ordovician age. By contrast, at Barlings Beach, basalt is associated with highly disrupted chert (tectonic mélange), various slivers of mudstone and turbidites, and turbidites of the Adaminaby Group. Immobile elements in the basalts show consistent patterns that allow the magmatic affinity and tectonic setting to be determined in spite of pervasive hydrothermal alteration and subsequent lower greenschist facies metamorphism that accompanied strong folding and multiple foliation development. The Melville Point basalts show Ti/V ratios transitional between arc and MORB and therefore may have formed in either a forearc or backarc basin setting. However, these rocks have higher Ti/V ratios, LREE, Th and Nb than found in forearc basalts and are therefore considered to have formed in a backarc basin setting. In contrast to Melville Point, most basalts at Barlings Beach have a geochemical signature distinctive of ocean island settings like those reported from elsewhere in the Wagonga Group. We believe these rocks developed in a Cambrian backarc basin setting. In the Early to Middle Ordovician, much of the ocean basin was inundated by quartzose turbidites followed by basin destruction with accretion/underplating at a Late Ordovician–early Silurian Benambran subduction zone and formation of the Narooma Accretionary Complex.

KEY WORDS: Backarc basin basalt, Cambrian, Lachlan Orogen, ocean island basalt, Ordovician, Narooma Accretionary Complex, New South Wales, subduction

INTRODUCTION

Ordovician quartzose turbidites are widespread in the Lachlan Orogen of southeastern Australia (Figure 1) and formed in a deep-marine setting inundated by a huge turbidite submarine fan sourced from Gondwana (Fergusson & Coney 1992; Fergusson & Tye 1999; Fergusson *et al.* 2013). In spite of their structural complexity, many advances have been made in determining the stratigraphy of the Ordovician turbidite succession from graptolite ages in black shales of western Victoria (Willman 2007), and more widely elsewhere in the central and eastern Lachlan Orogen from conodont ages obtained from bedded chert/siliceous mudstone (<100 m thick) interbedded with the turbidite succession (Murray & Stewart 2001; Glen *et al.* 2009; Percival *et al.* 2011; Quinn *et al.* 2014). These stratigraphic studies have shown that turbidite and chert/black shale deposition was continuous throughout the Ordovician across much of the Lachlan Orogen, apart from the Macquarie Arc. They implied that a substantial ocean basin must have existed in the Cambrian prior to their deposition. Cambrian rocks are less widely exposed than Ordovician rocks and this has hindered their tectonic interpretation. Along margins of the Melbourne Zone in central Victoria, boninitic and tholeiitic mafic to intermediate volcanic rocks are overlain by Cambrian chert and shale that, at least locally, are conformably overlain by Ordovician turbidites (VandenBerg *et al.* 2000; Crawford *et al.* 2003a). In the Stawell Zone of western Victoria, backarc basin basalts are overlain by a thin unit of black shale of middle Cambrian age and in turn overlain by Cambrian quartzose turbidites (Squire & Wilson 2005). This association indicates development of basement to the Ordovician turbidites in West Pacific-style supra-subduction zone and backarc basin settings (Crawford *et al.* 2003a, b; Glen 2013) rather than oceanic crust formed at a mid-ocean ridge.

Cambrian rocks are also exposed on the New South Wales south coast in the Batemans Bay region (Figure 2) where the Wagonga Group contains basalt clasts and a basaltic breccia unit associated with middle to upper Cambrian shallow marine limestone (Bischoff & Prendergast 1987). A geochemical study of the basalts at Batemans Bay and Narooma reveals an ocean island basalt (OIB) character (Prendergast & Offler 2012). The association of OIB and shallow marine limestone is consistent with the earlier interpretation of a seamount that had been accreted to a subduction complex in the Ordovician to early Silurian (Bischoff & Prendergast 1987). Both the Wagonga Group and Ordovician turbidites (Adaminaby Group) are part of the Narooma Accretionary Complex that was formed in this subduction episode (Powell 1983a, b; Miller & Gray 1996, 1997; Offler *et al.* 1998; Fergusson & Frikken 2003; Prendergast 2007; Prendergast *et al.* 2011, 2012). The Narooma Accretionary Complex is marked by intense deformation with tight folds, abundant faults and disrupted rocks such as mélange of olistostromal, diapiric and/or tectonic origin. An alternative view is that the Wagonga Group rocks are the "Narooma terrane" developed in an oceanic setting distant from the Ordovician turbidite succession and subsequently accreted in a transpressional transform setting (Glen *et al.* 2004, 2009; Percival *et al.* 2011). A geochemical study of bedded cherts in the Narooma region has lent support to the idea that these rocks were deposited in an outer deeper ocean part of the Gondwana plate rather than on a separate advancing oceanic plate (Bruce & Percival 2014).

In this account, we report additional geochemical data from altered basalts in Wagonga Group rocks 20 km south of Batemans Bay, at Melville Point and Barlings Beach in the Tomakin area. These localities provide an insight into the stratigraphic relationships in the Narooma Accretionary Complex and illustrate the complexities that arise in these rocks. At Melville Point, a massive basaltic unit in the Wagonga Group is conformably overlain by chert and mudstone of the Narooma Chert, which in

turn, is conformably overlain by thick-bedded quartz-lithic sandstone turbidites of the basal Adaminaby Group (Etheridge *et al.* 1973; Powell 1983a; Fergusson & Frikken 2003; Prendergast 2007, figure 3; Fergusson *et al.* 2013). We have found that altered basalts at Melville Point have a backarc basin geochemical signature and discuss the significance of this finding in terms of the Cambrian oceanic basement of the Ordovician turbidites. In contrast, exposures at the eastern end of Barlings Beach, only 1 km east of Melville Point, are more disrupted and contain tectonic mélange and many discontinuous fault slivers. This has resulted in structural and stratigraphic complexity but still preserve elements of the same stratigraphic succession exposed at Melville Point. Basalts within these exposures have mainly an OIB setting consistent with the findings of Prendergast & Offler (2012) elsewhere in the Wagonga Group.

GEOLOGIC SETTING

The Lachlan Orogen along the New South Wales south coast consists of a widespread deformed basement of Ordovician quartzose turbidites of the Adaminaby Group, with much less common mainly Upper Ordovician black shale (Bendoc Group), and a coastal unit of the middle Cambrian to Ordovician Wagonga Group containing the Kianga Basalt, Narooma Chert and Bogolo Formation (Lewis *et al.* 1994). The Wagonga Group is developed in the Narooma region where it has been studied in detail by Glen *et al.* (2004) and shown to consist of numerous fault slices with middle Cambrian to Upper Ordovician units of chert and/or siliceous mudstone with an upper conformable and/or gradational boundary to a unit of mudstone and conglomerate (Bogolo Formation). The major structure was mapped as a northward plunging anticlinorium by Wilson (1968) but recognised by Miller & Gray (1996, 1997) as an "apparent antiformal structure" containing imbricated successions. Alternatively, Glen *et al.* (2004) inferred that the major structure is a south-plunging synform with its core occupied by the Bogolo Formation. Maps and cross sections in Glen *et al.* (2004) show tightly folded cherts and abundant small faults with localised duplication of the succession. From the distribution of fossil localities and stratigraphic units they inferred the presence of nine main imbricate structural slices.

The Wagonga Group of the Batemans Bay region is well exposed along the coast between the basal Sydney Basin succession north of Batemans Bay and the Adaminaby Group at Tomakin (Figure 2). Far fewer fossil ages are known from the Batemans Bay region compared to Narooma. In contrast to Narooma, Adaminaby Group turbidites have been mapped within the belt of Wagonga Group rocks east of Tomakin (Fergusson & Frikken 2003). The Wagonga Group in the Batemans Bay region, as at Narooma, includes the Bogolo Formation and Narooma Chert as well as smaller areas of altered basalt (Kianga Basalt; Wilson 1968) but no longer considered to exist as a mappable unit by Glen *et al.* (2004). At Melville Point, both the Adaminaby Group turbidites and chert and altered basalt of the Wagonga Group have been mapped (Prendergast 2007) and considered to show the "oceanic" basement to the Adaminaby Group that is otherwise not known apart from exposures 380 km to the west-southwest in eastern Victoria at the Howqua River.

The Adaminaby and Wagonga groups are complexly deformed with abundant tight to isoclinal folds, overprinting fold phases, multiple foliations/cleavages, abundant small-scale faults including delicate syn-sedimentary faults lacking significant fault gouge, and late faults with quartz veins and fault breccia (Miller & Gray 1996, 1997; Glen *et al.* 2004; Fergusson & Frikken 2003; Prendergast 2007; Prendergast & Offler 2012). Disrupted rocks are referred to as mélange with variously sedimentary, tectonic and diapiric origins suggested (Festa *et al.* 2010), but in the Batemans Bay and Narooma regions the disrupted rocks show a strong tectonic overprint (Miller & Gray 1996, 1997; Fergusson &

Frikken 2003; Prendergast 2007). Timing of deformation has been hard to constrain although $^{40}Ar/^{39}Ar$ ages have been used to infer substantial deformation of Late Ordovician to early Silurian age as part of the Benambran Orogeny (Offler *et al.* 1998; Fergusson & Phillips 2001; Prendergast *et al.* 2011). Major deformation predated intrusion of Moruya suite granitoids in the Early Devonian (Prendergast *et al.* 2012). P–T conditions during deformation and metamorphism in the Batemans Bay region indicates a 15 km burial depth and a relatively low geothermal gradient (Prendergast *et al.* 2011, 2012).

MELVILLE POINT

The exposures at Melville Point (Figure 3) are well known because of the contact between a highly deformed unit of chert and mudstone (Narooma Chert) and overlying, steeply dipping, thick-bedded sandstone with thin-bedded mudstone and chert of the Adaminaby Group (Etheridge *et al.* 1973; Powell 1983a; Prendergast 2007). Detrital zircon ages from the sandstone turbidites at this locality are mainly in the ranges 600–500 Ma and 1200–1000 Ma similar to those reported from Ordovician turbidites elsewhere in the Lachlan Orogen (Fergusson *et al.* 2013). A latest Cambrian–earliest Ordovician age based on conodonts was found in a thin chert bed at the western end of the rock platform (Bischoff & Prendergast 1987) and indicate that only the basal part of the Adaminaby Group and the older part of the Wagonga Group are present. A conformable stratigraphic contact exists between the Wagonga Group cherts and overlying thick-bedded turbidites of the basal Adaminaby Group at Melville Point (Figure 5e). This is contrary to Glen *et al.* (2004, p. 875) who considered several possibilities including “imbrication of Adaminaby Group with rocks of the Narooma Terrane”.

The Narooma Chert (Figure 3) contains abundant upright to steep, west-inclined, tight to isoclinal, east-verging folds as well as west-dipping thrust faults. Locally, two generations of nearly coplanar folds are evident with associated axial plane cleavages (Powell 1983a). The base of the Narooma Chert is exposed in the cores of several narrow anticlines that occur west of the main, steep west-dipping contact of Narooma Chert-basalt in the eastern part of the rock platform (Figure 3). These folds indicate that the overall enveloping surface must dip moderately to the west in these rocks compared to the steep west dips evident throughout the Adaminaby Group rocks west of the Narooma Chert. The intensity of mesoscopic folding indicates substantial shortening (>60%) implying a relatively thin stratigraphic thickness (<15 m) for the Narooma Chert at this locality.

The main outcrop of basalt in the eastern part of the rock platform consists of three facies namely massive basalt, pillow basalt, and manganese-stained, siliceous mudstone. Massive basalt, a prominent ~30 m wide unit (Figure 3), is fine-grained, foliated with speckled-green, altered mineral inclusions and rare occurrences of thin siderite veins, green mineral veins and brown weathering, transitional to a more intensely foliated conglomerate layer in the west (Figure 4), with some intermittent thin cherty bands and possible volcanic rock fragments up to 20 cm long. Relic primary textures of highly altered ferromagnesian minerals, flattened amygdales and feldspar, are visible in thin sections of some samples (e.g. MN14, 15), however, no primary mineral has been preserved (Figure 5a, b). Two foliations (S_1 and S_2) defined by white mica as well as tight F_2 folds defined by opaque minerals, are visible in thin sections of the more highly deformed basalts. Relict hydrothermal quartz (Figure 5), titanite and altered magnetite are commonly present and may show fracturing and elongation. Locally small fine-grained aggregates of chlorite and yellowish brown crystals of chlorite–smectite and aggregates of illite–chlorite occur in the matrix. Prendergast & Offler (2012) recorded similar features in the basalts. Quantitative XRD analysis shows that the unit is dominated by secondary clay minerals (80%), predominantly illite–muscovite (65%), and chlorite

(10%), together with kaolin (6%; Stokes 2013). Along the western margin of the massive basalt unit, on the southern side of the headland, is an outcrop ~3 m wide of strongly flattened pillow lavas that are elongate within the strong, steep, west-dipping foliation (Figures 5c, d). The pillows are a darker green colour than the adjacent massive basalt and have lighter coloured inter-pillow material. Bedded manganese-stained siliceous fine-grained rock, ~30 cm wide, outcrops through the centre of the massive basalt unit (Figure 3).

Intervals of thin-bedded mudstone and chert are interbedded with the thick-bedded quartz-lithic sandstones west of the Narooma Chert–Adaminaby Group contact and in places rip-up clasts of thin-bedded mudstone abound in thick-bedded sandstone units. The thickest interval of chert–mudstone has an across strike width of 10 m. It is strongly deformed with abundant mesoscopic folds and numerous faults at low angles to bedding, but we have been unable to find evidence of a faulted contact at the base of this unit. Our interpretation is that succession at Melville Point represents facies interdigitation between the Adaminaby Group and the underlying Wagonga Group, which at Narooma and elsewhere in the Batemans Bay region, includes rocks the same age and younger than the Adaminaby Group turbidites (Glen *et al.* 2004).

BARLINGS BEACH

Rock platforms at the eastern end of Barlings Beach and surrounding Barlings Island to the south, have a similar rock assemblage to Melville Point although some significant differences exist (Figures 6, 7). These rocks were mapped by Frikken (1997) and Fergusson & Frikken (2003) but have been found to be more complicated than previously thought (Stokes 2013). A northerly trending basaltic unit 10 m wide is within the rock platform at the eastern end of Barlings Beach (Figure 6). The basalt is intensely altered with primary minerals replaced by mixed-layer clays, hydrothermal quartz and altered magnetite in varying proportions (Figure 8a). It has a strong, north-striking, near vertical foliation that microscopically consists of two cleavages (S_1 and S_2) defined by white mica. Chert occurs as mappable lenses west of this, but in contrast to Melville Point, the chert is disrupted (tectonic mélange) and has abundant lenticular, boudinaged chert fragments, 1 cm to 2.5 m in length and up to 40 cm wide, set in a siliceous mudstone matrix and aligned parallel to the steep foliation (Figure 8). Well-developed bedding seen at Melville Point is not preserved in these rocks. Locally the intense lenticular fabric in chert is folded about north-trending axes consistent with the lenticular fabric being an early structure (S_1 or pre-S_1) with refolding by the D_2 deformation of Prendergast (2007). These cherts continue south to the eastern half of Barlings Island and are in fault contact to the west with Adaminaby Group turbidites (Fergusson & Frikken 2003). Thus the same lithologic units are developed here as at Melville Point but are considerably more deformed with stratal disruption in the chert unit and faulted contacts between units.

In addition to basalt, chert and Adaminaby Group turbidites, amongst the disrupted chert, are units of laminated mudstone, massive mudstone, siliceous mudstone and units with interbedded, graded beds of lithic sandstone and mudstone that are younging to the west (Stokes 2013). The interbedded lithic sandstone and mudstone turbidites have individual sandstone beds up to 50 cm thick. In thin section, the lithic sandstone has poorly sorted subangular albite grains in a matrix of altered lithic fragments. The lenticular geometry of these units (Figure 7) is probably of tectonic origin as they have sharp contacts with disrupted chert and basalt. A north-plunging antiform occurs in laminated mudstone, siliceous mudstone and overlying disrupted chert (Figure 7). Several late faults marked by sand-filled gutters cut across the rock platform as shown by offset units across them (Figure 7). They

were considered by Frikken (1997) to have strike-slip displacement, although the faults themselves are too poorly exposed to allow the sense and direction of movement to be determined.

East of the basaltic unit is a ~3 m wide zone of mélange with black siliceous mudstone matrix with scattered, lenticular quartz sandstone fragments up to 0.5 m long and aligned in the foliation subparallel to that in the adjoining basalt. Discontinuous lenticular fragments and elongate injections of brown-weathered basalt up to 4 m long occur throughout this mélange (Figure 8b, c). East of this zone is a mixed brown-weathered mudstone with boudinaged, thin chert fragments that are locally tightly folded with axial planes subparallel to the main foliation. More basalt injections occur in the extreme northern part of the unit adjacent to the beach sand. The basalt injections indicate remobilisation of the altered basalt unit that was attributed to diapiric injection during early deformation involving initial accretion of the succession, as discussed by Fergusson & Frikken (2003) and illustrated in Fergusson (2014, figure 11). East of this mixed zone is black mudstone of the Narooma Chert and is characterised by abundant thin beds of white to grey mudstone, siltstone to very fine sandstone with plane lamination, rare micro-cross lamination and abundant variably oriented, small-scale, syn-sedimentary faults that both extend and duplicate bedding. The black mudstone is steeply dipping to the west with common east-verging tight mesoscopic folds with well-developed steep, west-dipping axial planar cleavage (Fergusson & Frikken 2003). No fossils have been found in this unit but further north along the coast Upper Ordovician graptolites have been found at two localities in black mudstone (Jenkins *et al.* 1982).

GEOCHEMISTRY – ALTERED BASALTS

Methods

Rock chips were ground to powders in a Tema mill with a chrome steel crusher. Major and trace elements were determined using ICP-OES and ICP-MS, respectively, by Genalysis Laboratory Services, Adelaide. Ni was determined by a SPECTRO XEPOS XRF at the University of Wollongong and loss on ignition (LOI) from 1 gm of sample heated at 1050°C.

Results

Major and trace element compositions, particularly the light lithophile elements (LILE) are variable owing to the intense deformation, alteration and recrystallisation the samples have undergone (Table 1). Much of the high concentration of LILE (e.g. Sr, Ba and K) and high loss on ignition (LOI = 6.05–11.06) is due to variation in the content of white mica. However, despite the intense alteration manifest in these samples, consistent and distinctive patterns are shown by immobile elements (Figures 9–13). In addition, when a variety of discrimination diagrams involving these immobile elements are applied, particular tectonic settings emerges for individual samples.

Zr/TiO_2 and Nb/Y ratios (Winchester & Floyd 1977) indicate that some rocks were derived from sub-alkaline, basaltic protoliths (Melville Point samples MPG2, MN12, MN13, MN14, MN15 and Barlings Beach sample BN32), others from alkaline basaltic protoliths (Barlings Beach samples BN1, BN2, BN36). For the former, TiO_2 is <2 wt% and >2 wt% for the latter. Further, with the exception of BN32, the sub-alkaline samples show light rare earth element (LREE) depleted and flat, heavy rare earth element (HREE) patterns with $(Ce/Yb)_N$ varying from 0.68 to 0.91, $(La/Sm)_N$ from 0.36 to 0.92, and $(Sm/Lu)_N$ from 1.12 to 2.35 (Table 1; Figure 9). By contrast, the alkaline samples are LREE enriched with $(Ce/Yb)_N$ varying from 7.0 to 9.6, $(La/Sm)_N$ from 3.78 to 4.87 and $(Sm/Lu)_N$ from 2.44 to 3.66. Rock/primitive-mantle normalised plots show coherent patterns and consistent high field strength

element (HFSE) concentrations with both groups showing higher Nb, Ta and Th contents than N-MORB, particularly for the alkaline samples (Figure 9). Depletion of Nb, Hf and Ti is a feature of BN32.

DISCUSSION

Geochemistry

Application of the discriminant diagrams proposed by Shervais (1982) and Cabanis & Lecolle (1989) reveal that most samples plot in the N-MORB or within plate fields (Figures 11, 12). By contrast, BN32 has the composition of a volcanic arc basalt and a composition transitional between calc-alkaline and tholeiitic arc basalts; MPG2 is a weakly enriched E-type MORB (Figure 12). Furthermore, the Ti/V ratios (Shervais 1982) of the sub-alkaline samples occur on the border between the arc and MORB fields (Figure 11) and thus have the composition of basalts transitional between those found in these settings. This suggests they may have formed either in a backarc or forearc setting. Both these types of basalts have N-MORB like affinities and plot in similar positions on the discrimination diagrams of Shervais (1982) and Cabanis & Lecolle (1989). Further, they plot in similar positions close to the MORB–OIB array on the Th/Yb–Nb/Yb diagram (Figure 13). Where they differ is most apparent on V–Ti, and primitive mantle normalised diagrams. On the former, forearc basin basalts (FAB) plot in the arc field because they have lower Ti/V ratios than backarc basin basalts (BAB; Figure 11). In the latter, FAB's exhibit lower LREE, Th and Nb contents than BAB (Figure 10b). Thus, it is concluded that they have formed in a backarc basin setting probably close to the spreading axis in view of their proximity to the MORB–OIB array on the Th/Yb–Nb/Yb diagram. It is noteworthy that all these samples come from Melville Point.

The samples with the alkali basaltic affinity have compositions typical of OIB, based on their primitive mantle and chondrite-normalised patterns, and on their La/Yb values that are >10 (Table 1; Condie *et al.* 2002). These samples all come from the Barlings Beach locality and are similar to those reported by Prendergast & Offler (2012) further east around Burrewarra Point.

The only sample to record an arc signature is BN32, an injected greenstone similar to BN36, which has an OIB affinity. Thus they have fundamentally different compositions but show similar field relationships.

Implications for Cambrian tectonic setting of the Tasmanides

Development of supra-subduction zone ophiolitic assemblages includes boninites that have been associated with the initiation of subduction zones (Stern *et al.* 2012). They are considered to be indicative of a West Pacific style of oceanic basin with island arcs and backarc basins, a scenario proposed for the Cambrian of the Lachlan and New England orogens (Crawford *et al.* 2003a, b; Glen 2013). Early Cambrian plagiogranite and boninite with ages of 536 Ma and 530 Ma from the Peel Fault system in northeastern New South Wales are the oldest component of this assemblage (Aitchison & Ireland 1995; Sano *et al.* 2004; Glen 2013). Given the very restricted nature of these rocks and the subsequent overprinting tectonic history, confident reconstruction of the original geometry of the associated convergent margin seems unlikely. Nevertheless, Glen (2013) has argued that this assemblage represents initiation of subduction in the paleo-Pacific Ocean neighbouring East Gondwana, and was followed by massive rollback to the east (in present-day co-ordinates) generating backarc basins and boninitic island arc crust.

Lower Cambrian fossils from the Heathcote Volcanics located at the eastern margin of the Bendigo Zone place a constraint on the formation of the boninitic igneous basement at *ca* 515 Ma (Glen 2013,

p. 331). The geometry of any subduction zone associated with these rocks is not apparent given that the structures that have exhumed them formed in the Benambran Orogeny at least 60 Ma after the age of the boninites. The boninitic–tholeiitic volcanic basement succession, at the eastern margin of the Melbourne Zone at the Howqua River, has poor age control (Fergusson 1998) whereas further southeast in the Dolodrook River, upper middle to lowermost upper Cambrian limestone olistoliths in the Garvey Gully Formation are associated with ultramafic rocks (Crawford *et al.* 2003a; Engelbretsen 2006). This is consistent with development of a possible oceanic transform fault segment within the oceanic setting (Spaggiari *et al.* 2003, 2004). By contrast, the Melbourne Zone had a continental substrate continuous with Tasmania and has most likely undergone northward translation along the East Gondwana margin (Cayley 2011). Emplacement of middle Cambrian supra-subduction ophiolite in Tasmania was attributed to east-dipping subduction (Berry & Crawford 1988) and was probably associated with emplacement of inferred ophiolite fragments in the eastern Melbourne Zone interpreted as responsible for magnetic highs reflecting a source at depths of 25–10 km (McLean *et al.* 2010). The boninitic–tholeiitic–ultramafic associations of the eastern Bendigo Zone and southwest Tabberabbera Zone reflect initial formation in an arc–forearc associated with subduction followed by generation of the tholeiitic basalts in a backarc basin (Crawford *et al.* 2003a). Backarc basin basalts also occur at the junction of the Stawell and Bendigo zones and in the western Stawell Zone of western Victoria (Crawford *et al.* 2003a).

What significance do the basalts in the Narooma Accretionary Complex have for our understanding of the Cambrian tectonic setting? The association of OIB and Middle to upper Cambrian limestone at Burrewarra Point (Bischoff & Prendergast 1987; Prendergast & Offler 2012) provides evidence for a seamount having developed in the Cambrian off the eastern margin of Gondwana, a view that is generally supported (Glen *et al.* 2004). Basalt clasts in the olistostromal mélange of the Bogolo Formation at Narooma were considered to be derived from the seamount and indicate its possible southward extent (Glen *et al.* 2004). At Burrewarra Point, the Cambrian basaltic breccia unit and associated limestones occur adjacent to and within disrupted quartz turbidites of the Adaminaby Group (Fergusson & Frikken 2003). At least in part this reflects secondary diapiric remobilisation and injection interpreted by Fergusson & Frikken (2003) as having formed during initial imbrication of the succession. They are not associated with chert and black mudstone of the Narooma Chert that are widely developed in the Batemans Bay region. In contrast, at Barlings Beach, the OIB occur with disrupted chert, distinctive lithic turbidites and associated mudstone. These lithic turbidites are relatively uncommon but have been found elsewhere in the Wagonga Group of the Batemans Bay region and were considered by Ralser (1981) to have been derived from erosion and redeposition of sand detritus from the seamount. Thus from Burrewarra Point west to Barlings Beach the relationships are consistent with a seamount in the east and with deep-water facies preserved at Barlings Beach to the west along the tapering flank of the seamount. Further west at Melville Point, the lack of OIB indicates preservation of igneous basement to the seamount deposit, which is backarc basin crust. Thus the Wagonga Group OIB reflects seamount(s) with development of a topographically elevated region of the ocean basin that because of its distal setting and elevation avoided subsequent Ordovician turbidite deposition in the Narooma region. Elsewhere in the Lachlan Orogen, Ordovician turbidite deposition is missing from the eastern Melbourne Zone and much of the Macquarie Arc but occurred everywhere else. We consider that the available exposure is too restricted for the Cambrian rocks to speculate on the number and geometry of the subduction zones that were associated with the development of these rocks. One puzzling aspect of the Lachlan and New England orogens are the widespread Cambrian boninitic assemblages indicating supra-subduction zone settings followed by backarc basin sea floor spreading. A modern analogy for this

setting is the present-day Philippine Sea plate, where backarc basin crust is presumably much more widespread than arc-related boninitic assemblages of the Izu–Bonin–Marianas island arc (Figure 14; Stern *et al.* 2012).

Implications for the Narooma Accretionary Zone

A subduction complex interpretation of the Narooma Accretionary Zone has been supported in the literature (Powell 1983a, b; Bischoff & Prendergast 1987; Miller & Gray 1996, 1997; Offler *et al.* 1998; Fergusson & Frikken 2003; Prendergast 2007; Prendergast et al. 2011, 2012) apart from Glen et al. (2004, 2009), Glen (2013) and Aitchison & Buckman (2012). The association of complexly deformed deep-marine chert, mudstone, turbidites, sedimentary/diapiric/tectonic mélange, seamount deposits, ocean island basalts, and backarc basin basalts, with imbrication of the succession mapped at Batemans Bay and Narooma, are aspects that are most consistent with a subduction complex setting. Additionally it has been argued on the basis of geothermal gradients of 20°/km at Batemans Bay and 26–35°/km at Narooma that these accord with a subduction complex setting (Offler *et al.* 1998; Prendergast *et al.* 2011, 2012).

The Melville Point locality is important as this is the only place in southeastern New South Wales where the basement to the Ordovician turbidite succession is exposed and furthermore has been shown to have a backarc setting from the geochemistry of the basalts in spite of their intense alteration. The overall eastward vergence of the main fold phase at Melville Point and the exposure of Adaminaby Group sandstones at the eastern end of the rock platform imply that the Melville Point Wagonga Group succession has been thrust to the east along an unexposed fault (Figure 3). The exposure of Adaminaby Group turbidites with disrupted chert and basalt at the eastern end of Barlings Beach and Barlings Island indicates duplication of these ocean-floor successions as is typical of subduction complexes (Kusky *et al.* 2013).

In the original models of subduction complex development as given in Karig & Sharman (1975), and discussed by many authors since (Kusky *et al.* 2013 and references therein), the accretionary pattern is shown by the imbrication of ocean floor stratigraphy resulting in units that young internally in the same direction towards the top of the structural pile (i.e. away from the site of the trench and subducting plate) with the stratigraphic range of ages in outer and later accreted slices getting progressively younger down the structural pile towards the trench and site of accretion (Figure 15). This pattern has not been demonstrated in the Narooma Accretionary Zone and only occurs on a large scale in the other Lachlan subduction complexes in western Victoria (Stawell and Bendigo zones) and the central Lachlan Orogen (Girilambone, Wagga–Omeo and Tabberabbera zones, Fergusson 2003, 2014). The reason for this is that subduction has occurred well after formation of the ocean basin, which occurred in the Cambrian at 540 to 500 Ma (Glen 2013), and deposition of the thick Lower to Middle Ordovician turbidite succession. The Ordovician turbidites were not deposited in a synsedimentary subduction trench, which is the analogue chosen by several authors for criticism of subduction complex models of the Lachlan Orogen (Aitchison & Buckman 2012; Glen 2013). Thus a thick ocean floor plate succession existed prior to subduction; whereas for turbidite sedimentation in the trench synchronous with subduction, these younging patterns are expected as presented in models of subduction complex development by Karig & Sharman (1975) and others (Figure 15). For the Narooma Accretionary Complex, subduction and accretion occurred in the Benambran Orogeny in the Late Ordovician to early Silurian. A thick subduction complex rapidly formed with imbrication of the pre-existing ocean plate stratigraphy, and development of associated shale diapirism and also some basaltic diapirism as evident at Burrewarra Point, Barlings Beach and elsewhere in the

Batemans region (Fergusson & Frikken 2003; Fergusson 2014). Much of the intense ductile deformation and late brittle deformation in these rocks reflects thickening of the subduction complex during underplating of initially accreted units at depths of 10 to 15 km (Offler *et al.* 1998; Fergusson & Frikken 2003; Prendergast *et al.* 2011, 2012). Because of the pre-existing thick turbidite succession, our present concept is that the subduction complex is dominated by these rocks and lacks evidence for the younging pattern shown by accretion of synorogenic trench–wedge turbidites (Figure 15). Additionally, the surficial levels of the subduction zone that may potentially preserve the younging pattern, with the highest layers in trenchward imbricated slices getting progressively younger, are unlikely to be preserved given the exhumation and resulting exposure of only deeper levels of the subduction complex.

CONCLUSIONS

Basalts in the Narooma Accretionary Complex are mainly of OIB-like character as shown previously by Prendergast & Offler (2012) and confirmed by our studies of samples from Barlings Beach, 20 km south of Batemans Bay. Additionally, we have found that the basement to Wagonga Group chert and mudstone and conformably overlying turbidites of the Adaminaby Group at Melville Point, 1 km west of Barlings Beach, consist of basalts formed in a backarc basin setting. The West Pacific style of ocean basement for the Cambrian developed over 40 Ma but the arrangement of associated subduction zones and directions of rollback remain difficult to establish given the lack of exposed Cambrian rocks through most of the Lachlan Orogen. Accretion and underplating of these Cambrian and overlying Ordovician turbidite fan oceanic successions has resulted in development of a subduction complex in the Late Ordovician–early Silurian Benambran Orogeny that lacks the detailed younging patterns of fault slices expected from the accretion of trench–wedge deposits formed synchronously with subduction.

ACKNOWLEDGEMENTS

Research support was provided by the GeoQuEST Research Centre, funded by the University of Wollongong. We appreciate the experience and assistance given by Brian Jones, Allen Nutman and Ryan Manton in regard to XRD, hand-held and laboratory XRF geochemistry. Ryan Manton and Solomon Buckman have helped us in the field. Discussions with all these researchers are gratefully acknowledged. Chris Owers, Heidi Brown and Alex Ullrich provided much advice on ArcGIS. Jose Abrantes (JA) and Yanyan Sun made thin sections and JA assisted with collection of XRD and XRF data. We thank David Gray and Gordon Packham for their constructive reviews of the manuscript.

REFERENCES

AITCHISON J. C. & BUCKMAN S. 2012. Accordion vs. quantum tectonics: Insights into continental growth processes from the Paleozoic of eastern Gondwana. *Gondwana Research* **22**, 674–680.

AITCHISON J. C. & IRELAND T. R. 1995. Age profile of ophiolitic rocks across the Late Palaeozoic New England Orogen, New South Wales: implications for tectonic models. *Australian Journal of Earth Sciences* **42**, 11–23.

AMANTE C. & EAKINS B. W. 2009. ETOPO1 a arc-minute global relief model: Procedures, data sources and analysis. *NOAA Technical Memorandum NESDIS NGDC-24,* 19 p.

BERRY R. F. & CRAWFORD A. J. 1988. The tectonic significance of Cambrian allochthonous mafic–ultramafic complexes in Tasmania. *Australian Journal of Earth Sciences* **35**, 523–533.

BISCHOFF G. C. O. & PRENDERGAST E. I. 1987. Newly discovered Middle and Late Cambrian fossils from the Wagonga Beds of New South Wales, Australia. *Neues Jahrbuch fur Geologie und Palaontologie* **175**, 39–64.

BRUCE M. C. & PERCIVAL I. G. 2014. Geochemical evidence for provenance of Ordovician cherts in southeastern Australia. *Australian Journal of Earth Sciences*, DOI: 10.1080/08120099.2014.956792.

CABANIS B. & LECOLLE M. 1989. Le diagramme La/10–Y/15–Nb/8: an outil pour la discrimination des series volcaniques et la mise en evidence des processus de mélange et /ou de contamination crustale. *Comptes Rendus de l'Academie des Sciences Series II* **309**, 2023–2029.

CAYLEY R. A. 2011. Exotic crustal block accretion to the eastern Gondwanaland margin in the Late Cambrian–Tasmania, the Selwyn Block, and implications for the Cambrian–Silurian evolution of the Ross, Delamerian, and Lachlan orogens. *Gondwana Research* **19**, 628–649.

CONDIE K. C., FREY B. A. & KERRICH R. 2002. The 1.75-Ga Iron King Volcanics in west central Arizona: a remnant of an accreted oceanic plateau derived from a mantle plume with a depleted component. *Lithos* **64**, 49–62.

CRAWFORD A. J., CAYLEY R. A., TAYLOR D. H., MORAND V. J., GRAY C. M., KEMP A. I. S., WOHLT K. E., VANDENBERG A. H. M., MOORE D. H., MAHER S., DIREEN N. G., EDWARDS J., DONAGHY A. G., ANDERSON J. A. & BLACK L. P. 2003a. Neoproterozoic and Cambrian continental rifting, continent–arc collision and post-collisional magmatism. *In:* Birch W. ed. *The Geology of Victoria*, pp. 73–93. Geological Society of Australia, Victorian Division.

CRAWFORD A. J., MEFFRE S. & SYMONDS P. A. 2003b. 130 to 0 Ma tectonic evolution of the southwest Pacific and analogous geological evolution of the 600 to 220 Ma Tasman Fold Belt System. *In:* Hillis R. R. & Mueller R. D. eds. *Evolution and Dynamics of the Australian Plate*, pp. 383–403. *Special Publication 22 Geological Society of Australia & Special Paper 372 Geological Society of America*.

ENGELBRETSEN M. J. 2006. Early Late Cambrian lingulate brachiopods from the Dolodrook River limestones, eastern Victoria. *Memoirs of the Association of Australasian Palaeontologists* **32**, 225–246.

ETHERIDGE M. A., RANSOM D. M., WILLIAMS P. F. & WILSON C. J. L. 1973. Structural evidence of the age of folded rocks on the South Coast of New South Wales. *Journal of the Geological Society of Australia* **19**, 465–470.

FERGUSSON C. L. 1998. Cambrian–Silurian oceanic rocks, upper Howqua River, eastern Victoria: tectonic implications. *Australian Journal of Earth Sciences* **45**, 633–644.

FERGUSSON C. L. 2003. Ordovician–Silurian accretion tectonics of the Lachlan Fold Belt, southeastern Australia. *Australian Journal of Earth Sciences* **50**, 475–490.

FERGUSSON C. L. 2014. Late Ordovician to mid-Silurian Benambran subduction zones in the Lachlan Orogen, southeastern Australia. *Australian Journal of Earth Sciences* **61**, 587–606.

FERGUSSON C. L. & CONEY P. J. 1992. Implications of a Bengal Fan-type deposit in the Paleozoic Lachlan fold belt of southeastern Australia. *Geology* **20**, 1047–1049.

FERGUSSON C. L. & FRIKKEN P. 2003. Diapirism and structural thickening in an Early Palaeozoic subduction complex, southeastern New South Wales, Australia. *Journal of Structural Geology* **25**, 43–58.

FERGUSSON C. L. & PHILLIPS D. 2001. $^{40}Ar/^{39}Ar$ and K–Ar age constraints on the timing of regional deformation, south coast of New South Wales, Lachlan Fold Belt: problems and implications. *Australian Journal of Earth Sciences* **48**, 395–408.

FERGUSSON C. L. & TYE S. C. 1999. Provenance of Early Palaeozoic sandstones, southeastern Australia, part 1: vertical changes through the Bengal fan-type deposit. *Sedimentary Geology* **125**, 135–151.

FERGUSSON C. L., NUTMAN A. P., KAMIICHI T. & HIDAKA H. 2013. Evolution of a Cambrian active continental margin: the Delamerian–Lachlan connection in southeastern Australia from a zircon perspective. *Gondwana Research* **24**, 1051–1066.

FESTA A., PINI G. A., DILEK Y. & CODEGONE G. 2010. Mélanges and mélange forming processes: a historical overview and new concepts. *International Geology Review* **52**, 1040–1105.

FRIKKEN P. 1997. The stratigraphy and structure of the Early Palaeozoic succession – Burrewarra Point, southeastern NSW. Unpub. BSc (Hons) thesis, University of Wollongong, Wollongong.

GEOSCIENCE AUSTRALIA 2010. Surface Geology of Australia 1:1,000,000 scale data package. http://www.ga.gov.au/minerals/research/national/nat_maps/nat_geol_maps.jsp

GLEN R. A. 2013. Refining accretionary orogen models for the Tasmanides of eastern Australia. *Australian Journal of Earth Sciences* **60**, 315–370.

GLEN R. A., PERCIVAL I. G. & QUINN C. D. 2009. Ordovician continental margin terranes in the Lachlan Orogen, Australia: implications for tectonics in an accretionary orogen along the east Gondwana margin. *Tectonics* **28**, TC6012, http://dx.doi.org/10.1029/2009TC002446.

GLEN R. A., STEWART I. R. & PERCIVAL I. G. 2004. Narooma Terrane: implications for the construction of the outboard part of the Lachlan Orogen. *Australian Journal of Earth Sciences* **51**, 859–884.

JENKINS C. J., KIDD P. R. & MILLS K. J. 1982. Upper Ordovician graptolites from the Wagonga Beds near Batemans Bay, New South Wales. *Journal of the Geological Society of Australia* **29**, 367–373.

KARIG D. E. & SHARMAN G. F. 1975. Subduction and accretion in trenches. *Geological Society of America Bulletin* **86**, 377–389.

KUSKY T. M., WINDLEY B. F., SAFONOVA I., WAKITA K., WAKABAYASHI J., POLAT A. & SANTOSH M. 2013. Recognition of ocean plate stratigraphy in accretionary orogens through Earth history: A record of 3.8 billion years of sea floor spreading, subduction, and accretion. *Gondwana Research* **24**, 501–547.

LEAT P. T., PEARCE J. A., BARKER P. F., MILLAR I. L., BARRY T. L. & LARTER R. D. 2004. Magma genesis and mantle flow at a subducting slab edge: the South Sandwich arc–basin system. *Earth and Planetary Science Letters* **227**, 17–35.

LEWIS P. C., GLEN R. A., PRATT G. W. & CLARKE I. 1994. Explanatory Notes: Bega – Mallacoota 1:250,000 Geological Sheet, SJ/55-4, SJ/55-8. Geological Survey of New South Wales.

McLean M. A., Morand V. J. & Cayley R. A. 2010. Gravity and magnetic modelling of crustal structure in central Victoria: what lies under the Melbourne Zone? *Australian Journal of Earth Sciences* **57**, 153–173.

Miller J. McL. & Gray D. R. 1996. Structural signature of sediment subduction–accretion in a Palaeozoic accretionary complex, southeastern Australia. *Journal of Structural Geology* **18**, 1245–1258.

Miller J. McL. & Gray D. R. 1997. Subduction-related deformation and the Narooma Anticlinorium, eastern Lachlan Fold Belt. *Australian Journal of Earth Sciences* **44**, 237–251.

Murray S. I. & Stewart I. R. 2001. Palaeogeographic significance of Ordovician conodonts in the Lachlan Fold Belt, southeastern Australia. *Historical Biology* **15**, 145–170.

Offler R., Miller J. McL., Gray D. R., Foster D. A. & Bale R. 1998. Crystallinity and b_0 spacing of K-white micas in a Paleozoic accretionary complex, eastern Australia: metamorphism, paleogeotherms, and structural style of an underplated sequence. *Journal of Geology* **106**, 495–509.

Pearce J. A. 2008. Geochemical fingerprinting of oceanic basalts with applications to ophiolite classification and the search for Archean oceanic crust. *Lithos* **100**, 14–48.

Percival I. G., Quinn C. D. & Glen R. A. 2011. Review of Cambrian and Ordovician stratigraphy in New South Wales. *Quarterly Notes of the Geological Survey of New South Wales* **137**, 1–39.

Powell C. McA. 1983a. Geology of the New South Wales South Coast and adjacent Victoria with emphasis on the pre-Permian structural history. Geological Society of Australia, Specialist Group in Tectonics and Structural Geology Field Guide **1**, 118 pp.

Powell C. McA. 1983b. Tectonic relationship between the Late Ordovician and Late Silurian palaeogeographies of southeastern Australia. *Journal of the Geological Society of Australia* **30**, 353–373.

Prendergast E. I. 2007. Early Palaeozoic subduction in the southeastern Lachlan Fold Belt, Batemans Bay, New South Wales. *Australian Journal of Earth Sciences* **54**, 481–501.

Prendergast E. & Offler R. 2012. Underplated seamount in the Narooma accretionary complex, NSW, Australia. *Lithos* **154**, 224–234.

Prendergast E., Offler R., Phillips D. & Zwingman H. 2011. $^{40}Ar/^{39}Ar$ and K–Ar ages: Early Paleozoic metamorphism and deformation in the Narooma accretionary complex, NSW. *Australian Journal of Earth Sciences* **58**, 21–32.

Prendergast E., Offler R. & Zwingman H. 2012. Adaminaby Group west of Batemans Bay: Deformation and metamorphism of the Narooma accretionary complex, NSW. *Australian Journal of Earth Sciences* **59**, 1049–1066.

Quinn C. D., Percival I. G., Glen R. A. & Xiao W.-J. 2014. Ordovician marginal basin evolution near the palaeo-Pacific east Gondwana margin, Australia. *Journal of the Geological Society, London,* http://dx.doi.org/10.1144/jgs2012-034.

Ralser S. 1981. Palaeozoic geology of the Benanderah area, northeast of Batemans Bay, N.S.W. Unpub. B.Sc. (Hons) thesis, Australian National University, Canberra.

Reagan M. K., Ishizuka O., Stern R. J., Kelley K. A., Ohara Y., Blichert-Toft J., Bloomer S. H., Cash J., Fryer P., Hanan B. B., Hickey-Vargas R., Ishii T., Kimura J. I., Peate D. W., Rowe M. C. &

WOODS M. 2010. Fore-arc basalts and subduction initiation in the Izu–Bonin–Mariana system. *Geochemistry Geophysics Geosystems* **11**, Q03X12. doi:10.1029/2009GC002871.

SANO S., OFFLER R., HYODO H. & WATANABE T. 2004. Geochemistry and chronology of tectonic blocks in serpentinite mélange of the southern New England Fold Belt, NSW, Australia. *Gondwana Research* **7**, 817–831.

SHERVAIS J. W. 1982. Ti–V plots and the petrogenesis of modern and ophiolitic lavas. *Earth and Planetary Science Letters* **59**, 101–118.

SPAGGIARI C. V., GRAY D. R. & FOSTER D. A. 2003. Formation and emplacement of the Dolodrook serpentinite body, Lachlan Orogen, Victoria. *Australian Journal of Earth Sciences* **50**, 709–723.

SPAGGIARI C. V., GRAY D. R. & FOSTER D. A. 2004. Ophiolite accretion in the Lachlan Orogen, southeastern Australia. *Journal of Structural Geology* **26**, 87–112.

SQUIRE R. J. & WILSON C. J. L. 2005. Interaction between collisional orogenesis and convergent-margin processes: evolution of the Cambrian proto-Pacific margin of East Gondwana. *Journal of the Geological Society of London* **162**, 749–761.

STERN R. J., REAGAN M., ISHIZURA O., O'HARA Y. & WHATTAM S. 2012. To understand subduction initiation, study forearc crust: To understand forearc crust, study ophiolites. *Lithosphere* **4**, 469–483.

STOKES N. 2013. Relationships of mafic volcanic rocks and surrounding rocks in the inferred subduction complex, Batemans Bay district, southeastern New South Wales, Australia. Unpublished B.Sc.(Hons) Thesis, University of Wollongong, Wollongong. Available online: http://ro.uow.edu.au/thsci/60/

SUN S-S. & MCDONOUGH W. F. 1989. Chemical and isotopic systematics of oceanic basalts: implications for Mantle Compositions and Processes. *In:* Saunders, A.D., Norry, M.J. eds. *Magmatism in the Ocean Basins*, pp. 315–345. Geological Society of London, Special Publication **42**.

VANDENBERG A. H. M., WILLMAN C. E., MAHER S., SIMONS B. A., CAYLEY R. A., TAYLOR D. H., MORAND V. J., MOORE D. H. & RADOJKOVIC A. 2000. The Tasman Fold Belt System in Victoria. *Geology and mineralisation of Proterozoic to Carboniferous rocks.* Geological Survey of Victoria Special Publication.

WILLMAN C. E. 2007. Regional structural controls of gold mineralisation, Bendigo and Castlemaine goldfields, central Victoria, Australia. *Mineralium Deposita* **42**, 449–463.

WINCHESTER J. A. & FLOYD P. A. 1977. Geochemical discrimination of different magma series and their differentiation products using immobile elements. *Chemical Geology* **20**, 325–343.

WILSON C. J. L. 1968. Geology of the Narooma area, N.S.W. *Journal and Proceedings of the Royal Society of New South Wales* **101**, 147–157.

Received; accepted 31 October 2014

FIGURE CAPTIONS

Figure 1 Map of mainland southeast Australia showing the main Cambrian–Ordovician units and structural zones of the Lachlan Orogen. Modified from Geoscience Australia digital Surface Geology of Australia 1:1 000 000 scale (Geoscience Australia 2010). Abbreviations: DR = Dolodrok River, HV = Heathcote Volcanics, HR = Howqua River.

Figure 2 Geological map of the New South Wales south coast between north of Batemans Bay and south of Narooma. Modified from the Geoscience Australia digital Surface Geology of Australia 1:1 000 000 scale (Geoscience Australia 2010).

Figure 3 Geological map of Melville Point showing structure, and location of stratigraphic columns (see Figure 4) and includes some structural data from Powell (1983a).

Figure 4 Stratigraphic columns for two cross sections from the uppermost part of basalt unit, Melville Point. The southern-most section (a) crosses ~E–W, starting location 35.119460S, 150.123463E. In (b) section crosses ~E–W on east side of headland, 5–10 m north of (a), starting location 35.109469S, 150.1234654E.

Figure 5 Photographs of thin sections and exposures at Melville Point. (a) Thin section (crosspolarised light, MN15) with largely recrystallised groundmass of quartz, feldspar and less common chlorite in altered basalt transected by S1 and S2 cleavages defined by white mica. Altered opaque aggregates, oriented subparallel to S1, occur throughout. (b) Thin section (cross-polarised light, MN14) of altered basalt showing well developed foliations (S1 and S2) defined by white mica, flattened against titanite(?) aggregates. Matrix consists of fine-grained quartz and feldspar? (c) Flattened pillows in pillow lava. Pencil 18 cm long. (d) Folded and partly irregular (erosive) contact (dashed black line) between quartz-lithic sandstone layer of the basal Adaminaby Group and underlying thin-bedded mudstone and chert of the Wagonga Group. Geological hammer for scale (in ellipse).

Figure 6 Map of the headland at the eastern end of Barlings Beach including Barlings Island (based on mapping by Frikken 1997; Fergusson & Frikken 2003; Stokes 2013).

Figure 7 Detailed map of part of the rock platform at the eastern end of Barlings Beach. See Figure 6 for location.

Figure 8 (a) Photograph of sample BN1 (cross-polarised light) from Barlings Beach showing two foliations (S_1 and S_2) defined by white mica and relict, hydrothermal quartz aggregates (Q). (b) Brown-weathered altered basalt injected into black chert–siliceous mudstone on the eastern side of the basaltic unit at Barlings Beach. Geological hammer for scale. (c) Detail of basalt (B) injection into black chert–siliceous mudstone and small fragment of quartz sandstone (QS). Geological hammer for scale. (d) Lenticular fabric formed by chert fragments in mudstone matrix. White line outlines folded fabric around an F_2 fold. Hand-held GPS instrument for scale.

Figure 9 Chondrite-normalised patterns of all samples. 1 – BN1, 2 and 36 (OIB); 2 – BN32 (Arc); 3 – MN12, 13 (BAB); 4 – MN14, 15 (BAB); 5 – MPG2 (E-MORB). Normalising values from Sun & McDonough (1989).

Figure 10 Primitive mantle-normalised patterns based on immobile elements of: (a) alkaline and ARC (BN32) affinities; (b) sub-alkaline and forearc basalts (FAB). FAB data are from

Reagan *et al.* (2010). Note sub-alkaline samples have higher Th, Nb, Ti and LREE contents than FAB. Symbols as in Figure 9. Normalising values from Sun & McDonough (1989).

Figure 11 V *vs* Ti plot of Shervais (1982) showing majority of samples plotting in alkali basalt and MORB/BAB fields. Note sub-alkaline samples are juxtaposed against the ARC–OFB boundary and do not overlap with the FAB. Ti/V=10–20 Arc tholeiite; 20–50 MORB, BAB, Continental flood basalt; 50–100 Ocean island and alkali basalt. FAB data are from Reagan *et al.* (2010). Symbols as in Figure 9.

Figure 12 Y/15–La/10–Nb/8 diagram of Cabanis & Lecolle (1989) showing most samples plot in the alkali basalt or N-type MORB fields. Only BN32 plots in the arc field. 1A – calc-alkali basalts; 1C – volcanic arc tholeiites; 1B – overlap between 1A and 1C; 2A – continental basalts; 2B – backarc basin basalts; 3A – alkali basalts from intercontinental rift; 3B and 3C – E-type MORB; 3B – enriched; 3C – weakly enriched; 3D – N-type MORB.

Figure 13 Th/Yb–Nb/Yb plot for all samples. Fields for ARC and MORB–OIB from Leat *et al.* (2004) and Pearce (2008). Note most sub-alkaline samples plot in the BAB field and alkaline in the MORB–OIB array. By contrast BN32 plots in the arc field. **+** = data from Prendergast & Offler (2012).

Figure 14 Map of the Izu-Bonin-Marianas arc (IBM arc) and backarc basins of the northwest Pacific Ocean showing topography from ETOPO1 (Amante & Eakins 2009).

Figure 15 (a) Subduction complex model showing accretion of a relatively thin (<2 km) trench–wedge turbidites in a series of progressively younger thrust slices (from 1 = oldest, to 5 = youngest), adapted from Karig & Sharman (1975, figure 7a). (b) A more realistic model for the Narooma Accretionary Complex where accretion of a relatively thick succession on the subducting plate dominates the accretionary complex and results in repetition of the Lower to Middle Ordovician turbidites lacking evidence for accretion of younger turbidite slices as expected from accretion of trench–wedge turbidites. Thrusts are younger from left to right (1 = oldest, 3 = youngest).

Table 1 Geochemical data for altered basalts from Melville Point and the eastern end of Barlings Beach.

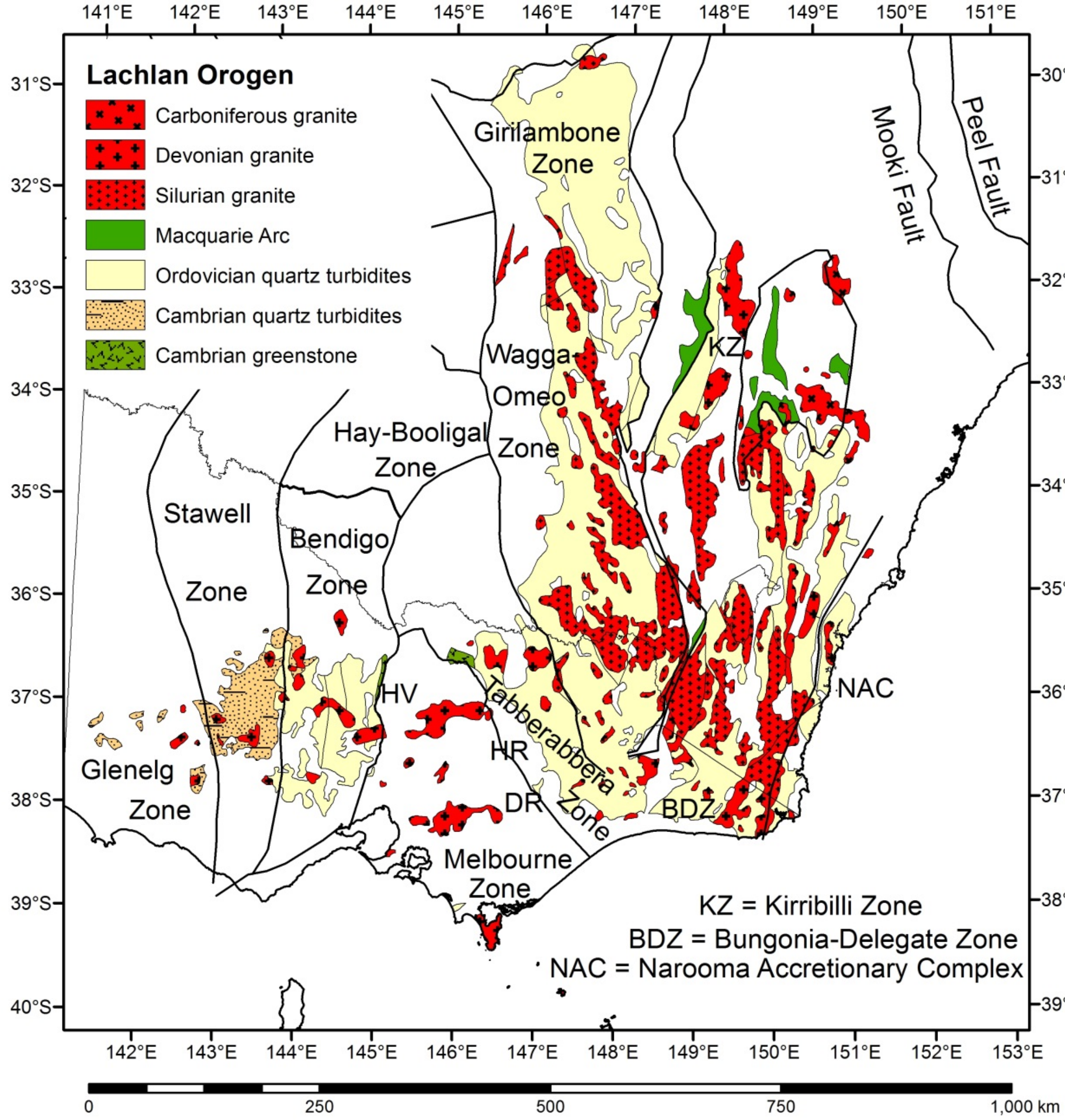
Lachlan Orogen
Carboniferous granite
Devonian granite
Silurian granite
Macquarie Arc
Ordovician quartz turbidites
Cambrian quartz turbidites
Cambrian greenstone
Girilambone Zone
Wagga-Omeo Zone
Hay-Booligal Zone
Stawell Zone
Bendigo Zone
Glenelg Zone
Melbourne Zone
Tabberabbera Zone
HV
HR
DR
KZ
BDZ
NAC
Mooki Fault
Peel Fault
KZ = Kirribilli Zone
BDZ = Bungonia-Delegate Zone
NAC = Narooma Accretionary Complex
0
250
500
750
1,000 km

Figure 1.

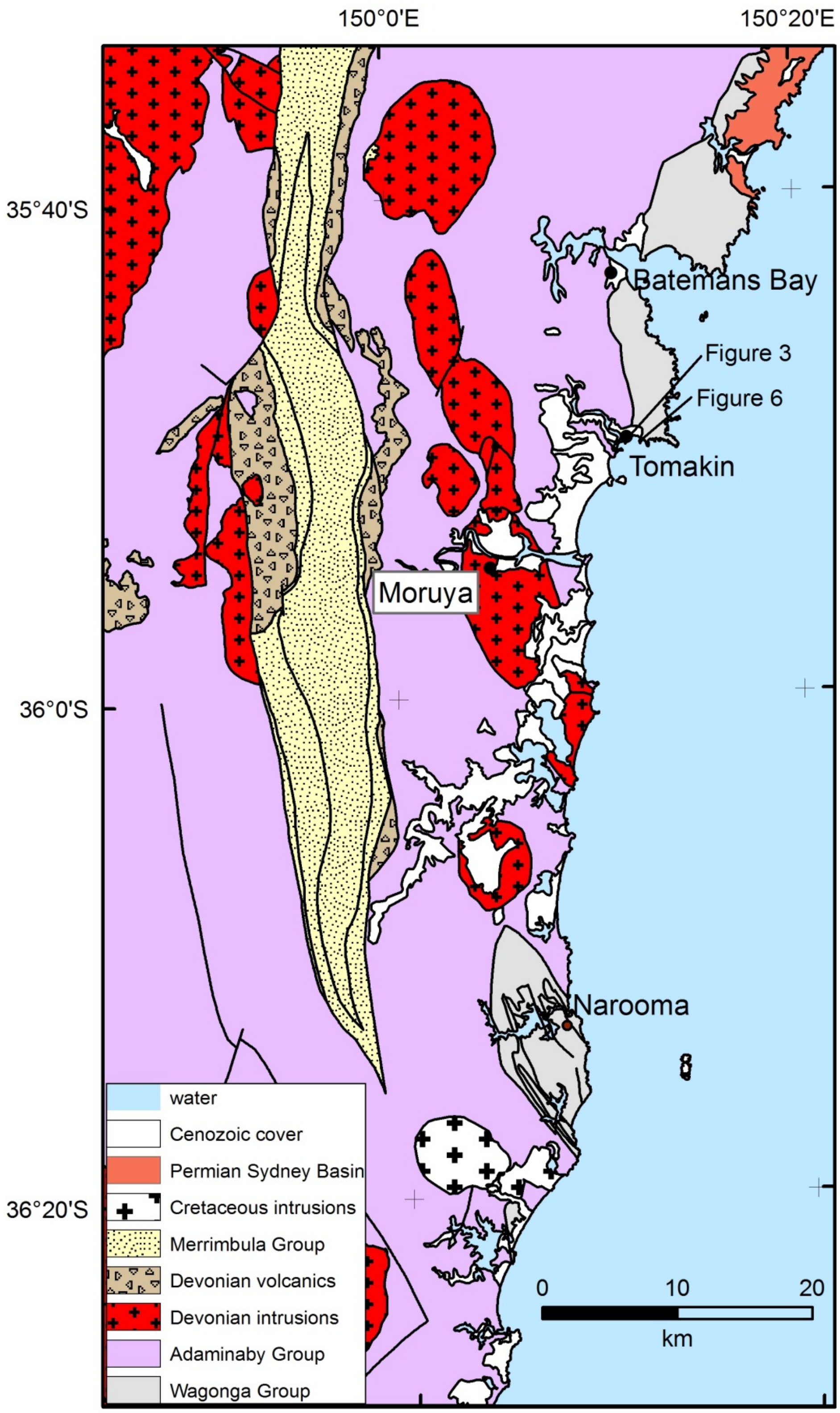
150°0'E
150°20'E
35°40'S
36°0'S
36°20'S
Batemans Bay
Figure 3
Figure 6
Tomakin
Moruya
Narooma
water
Cenozoic cover
Permian Sydney Basin
Cretaceous intrusions
Merrimbula Group
Devonian volcanics
Devonian intrusions
Adaminaby Group
Wagonga Group
0
10
20
km

Figure 2.

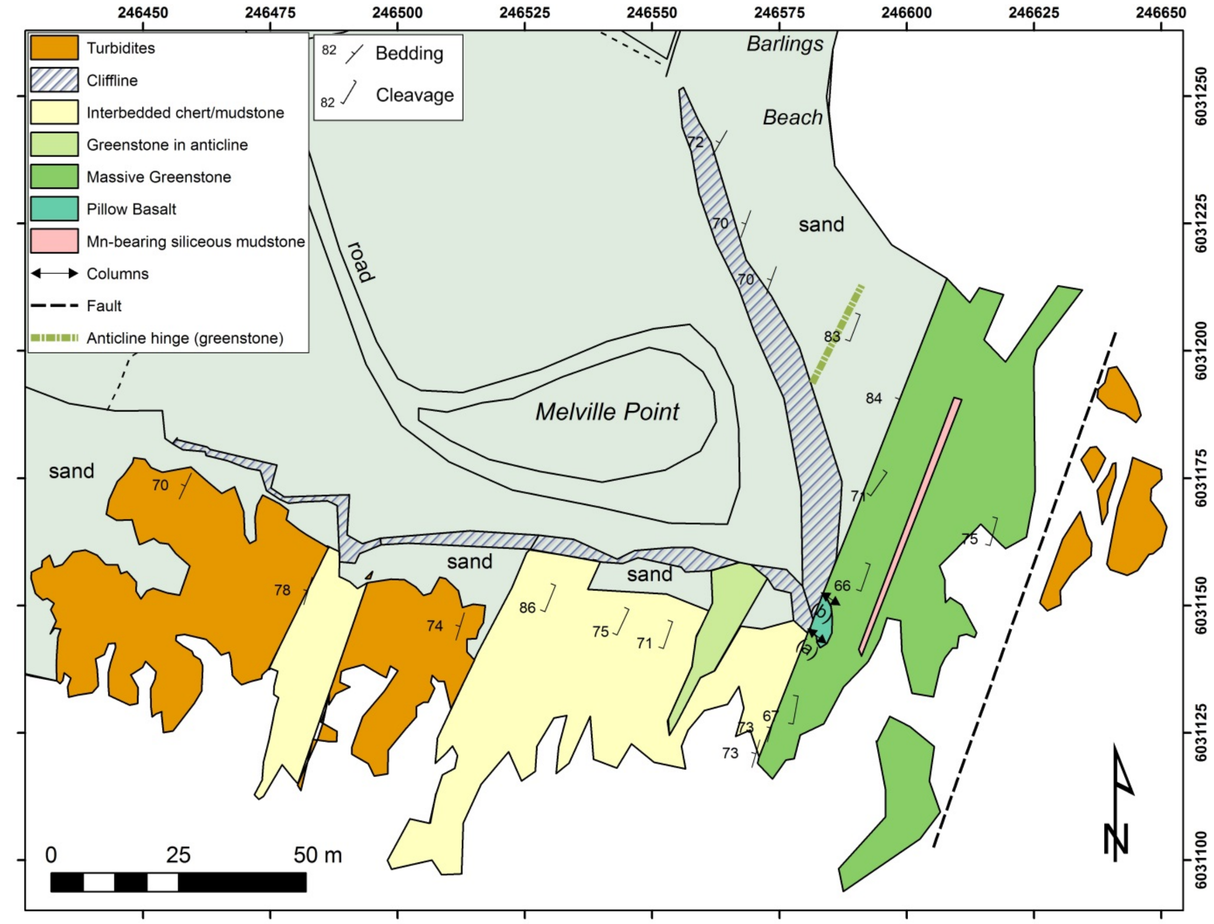
246450
246475
246500
246525
246550
246575
246600
246625
246650
6031250
6031225
6031200
6031175
6031150
6031125
6031100
Turbidites
Cliffline
Interbedded chert/mudstone
Greenstone in anticline
Massive Greenstone
Pillow Basalt
Mn-bearing siliceous mudstone
Columns
Fault
Anticline hinge (greenstone)
82 Bedding
82 Cleavage
Barlings
Beach
sand
road
Melville Point
sand
sand
sand
0
25
50 m
N

Figure 3.

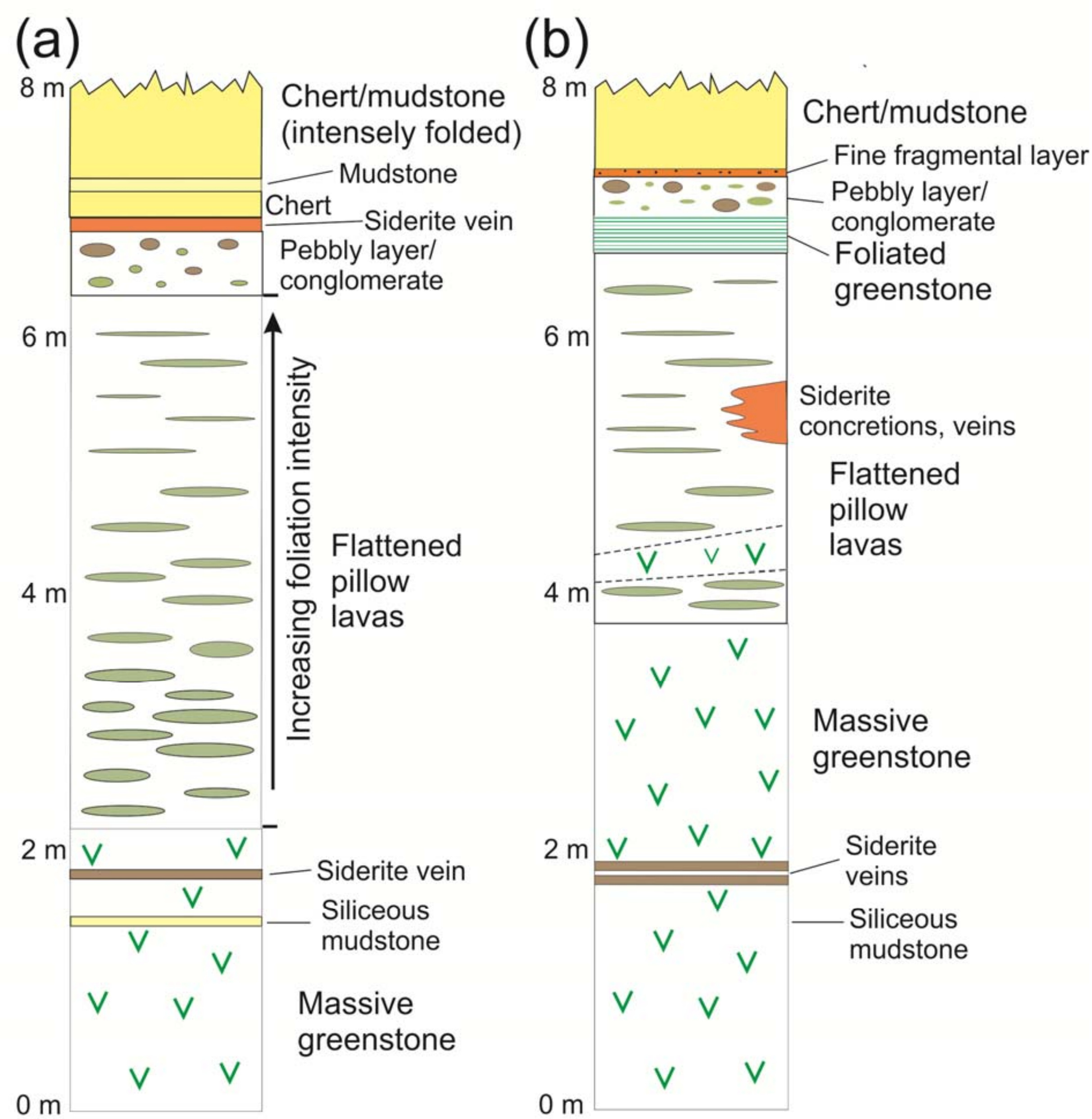

(a)
8 m
Chert/mudstone (intensely folded)
Mudstone
Chert
Siderite vein
Pebbly layer/ conglomerate
6 m
Increasing foliation intensity
Flattened pillow lavas
4 m
2 m
Siderite vein
Siliceous mudstone
Massive greenstone
0 m
(b)
8 m
Chert/mudstone
Fine fragmental layer
Pebbly layer/ conglomerate
Foliated greenstone
6 m
Siderite concretions, veins
Flattened pillow lavas
4 m
Massive greenstone
2 m
Siderite veins
Siliceous mudstone
0 m

Figure 4.

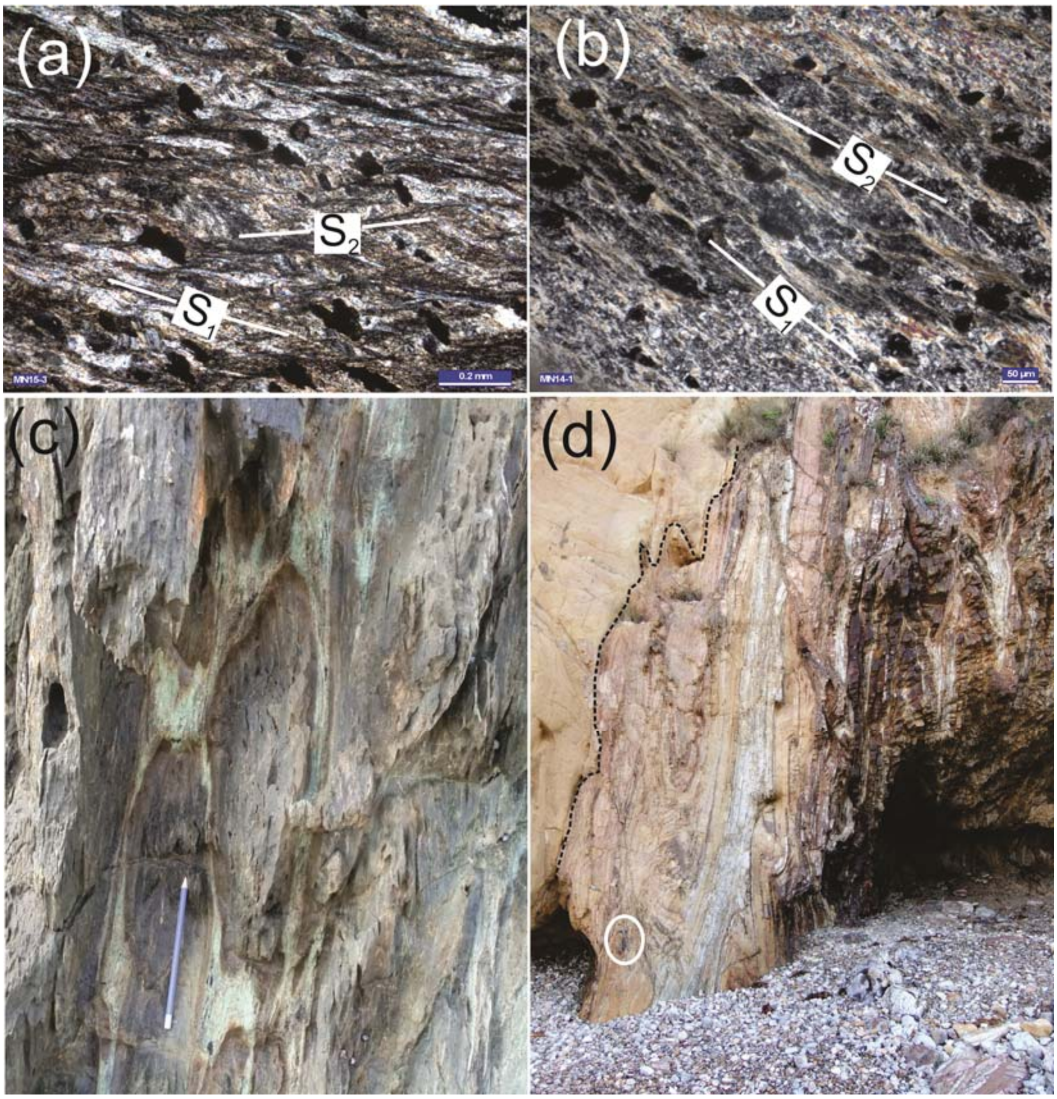

Figure 5.

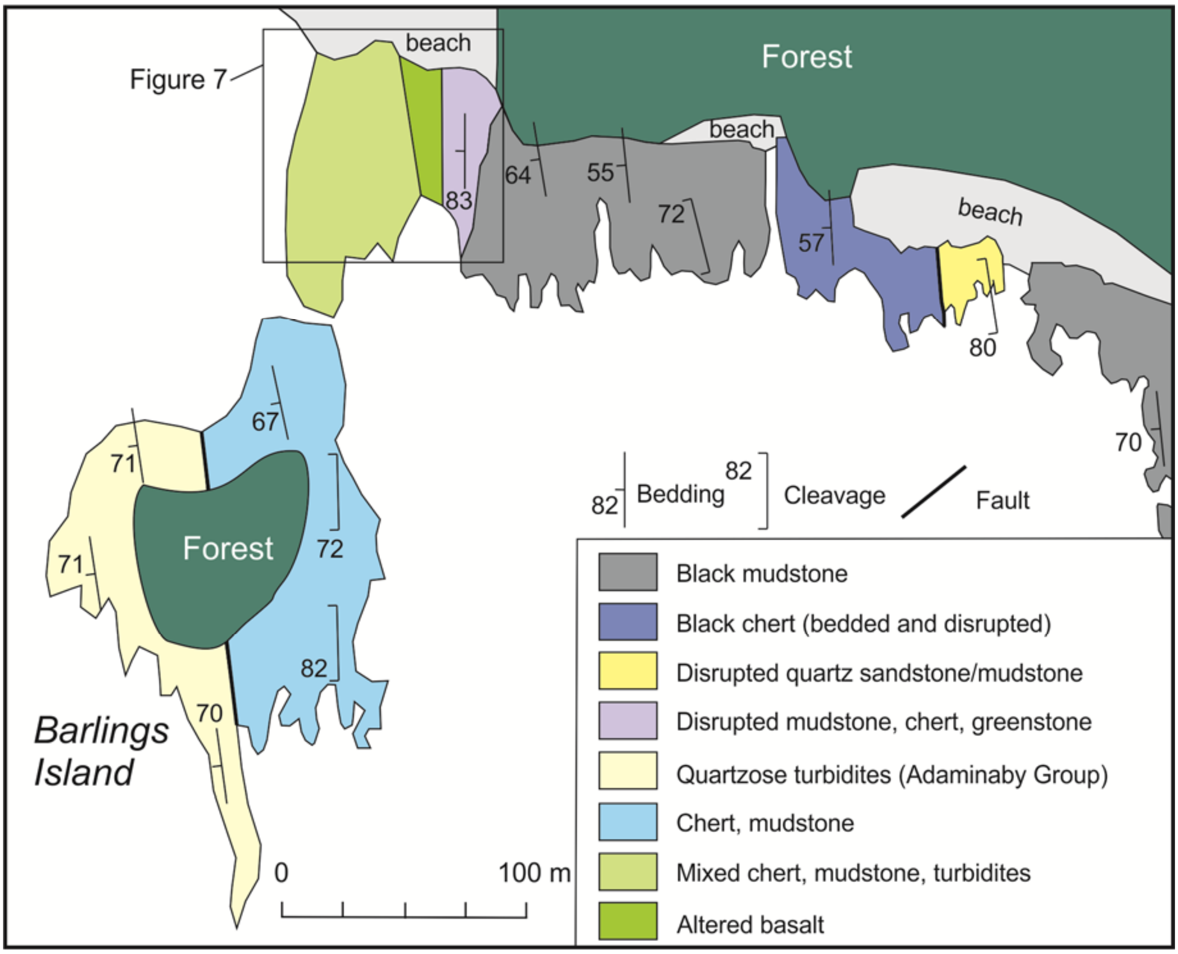
Figure 7
beach
Forest
beach
beach
83
64
55
72
57
80
70
67
71
71
Forest
72
82
70
Barlings Island
82 Bedding
82 Cleavage
Fault
0
100 m
Black mudstone
Black chert (bedded and disrupted)
Disrupted quartz sandstone/mudstone
Disrupted mudstone, chert, greenstone
Quartzose turbidites (Adaminaby Group)
Chert, mudstone
Mixed chert, mudstone, turbidites
Altered basalt

Figure 6.

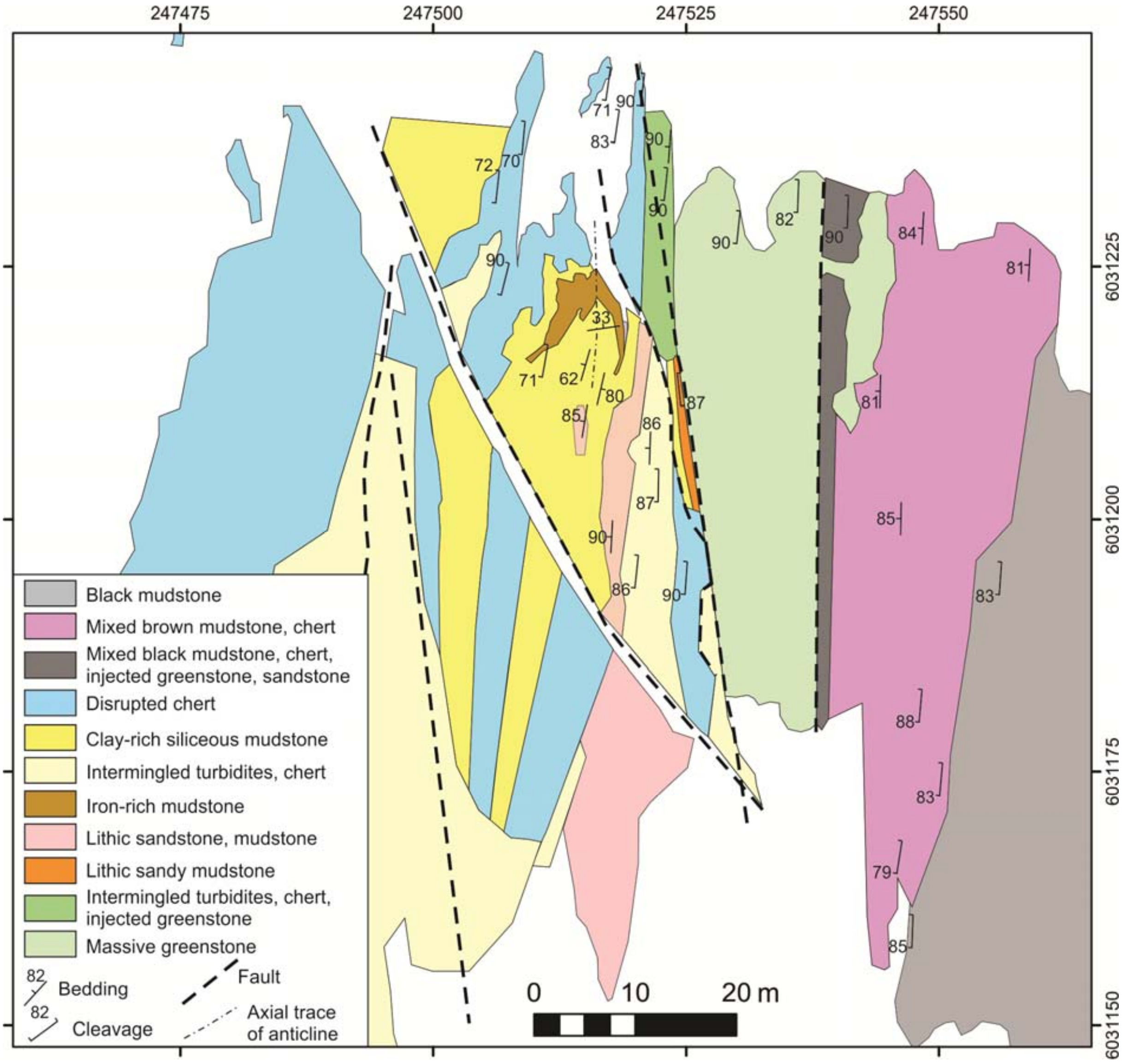
247475
247500
247525
247550
6031225
6031200
6031175
6031150
Black mudstone
Mixed brown mudstone, chert
Mixed black mudstone, chert, injected greenstone, sandstone
Disrupted chert
Clay-rich siliceous mudstone
Intermingled turbidites, chert
Iron-rich mudstone
Lithic sandstone, mudstone
Lithic sandy mudstone
Intermingled turbidites, chert, injected greenstone
Massive greenstone
82 Bedding
82 Cleavage
Fault
Axial trace of anticline
0
10
20 m

Figure 7.

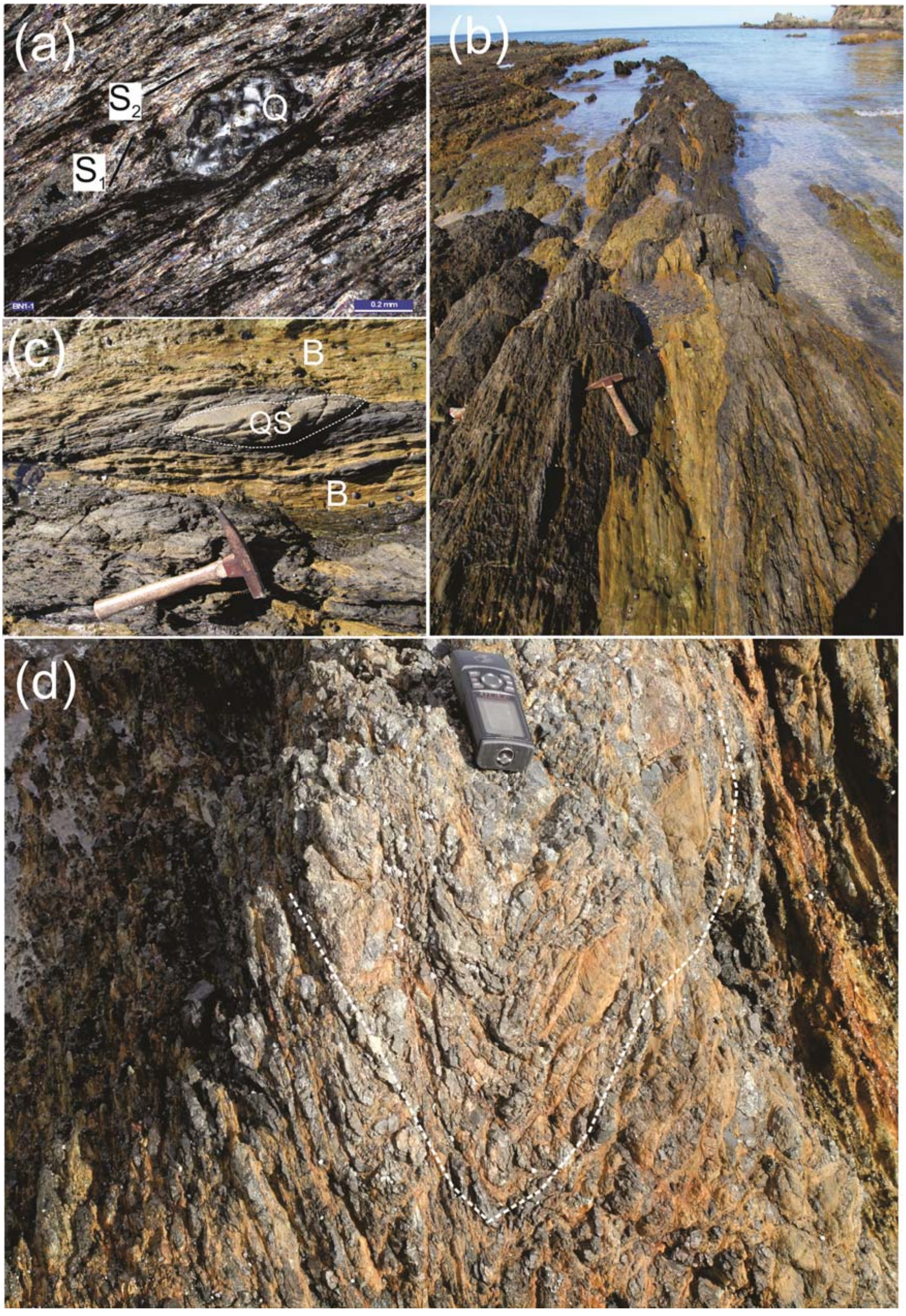

Figure 8.

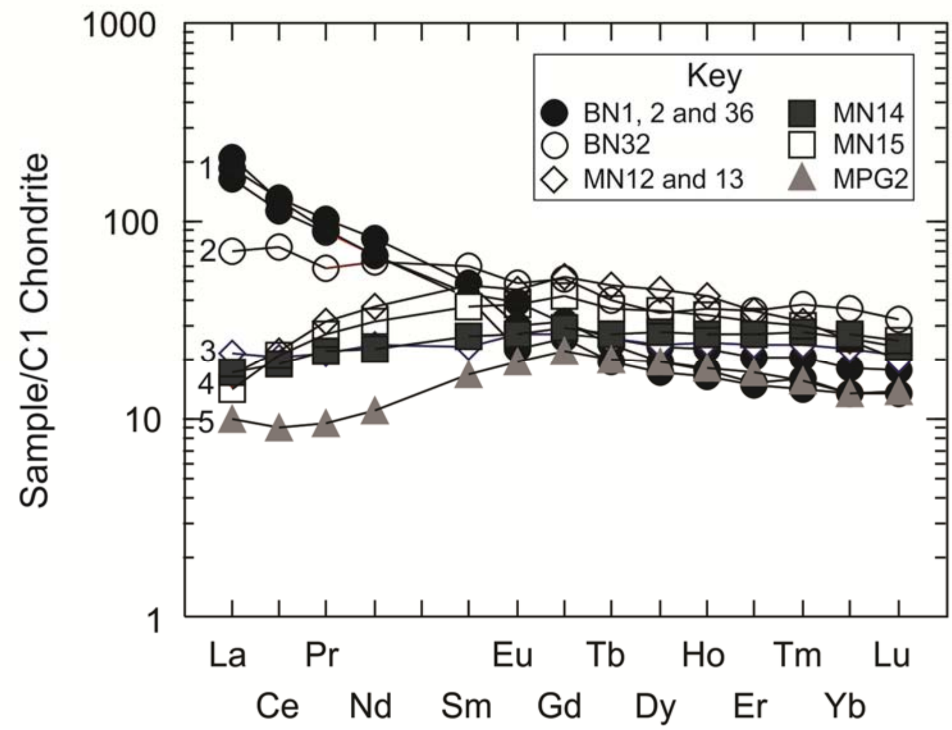
1000
100
10
1
Sample/C1 Chondrite
Key
BN1, 2 and 36
BN32
MN12 and 13
MN14
MN15
MPG2
1
2
3
4
5
La
Ce
Pr
Nd
Sm
Eu
Gd
Tb
Dy
Ho
Er
Tm
Yb
Lu

Figure 9.

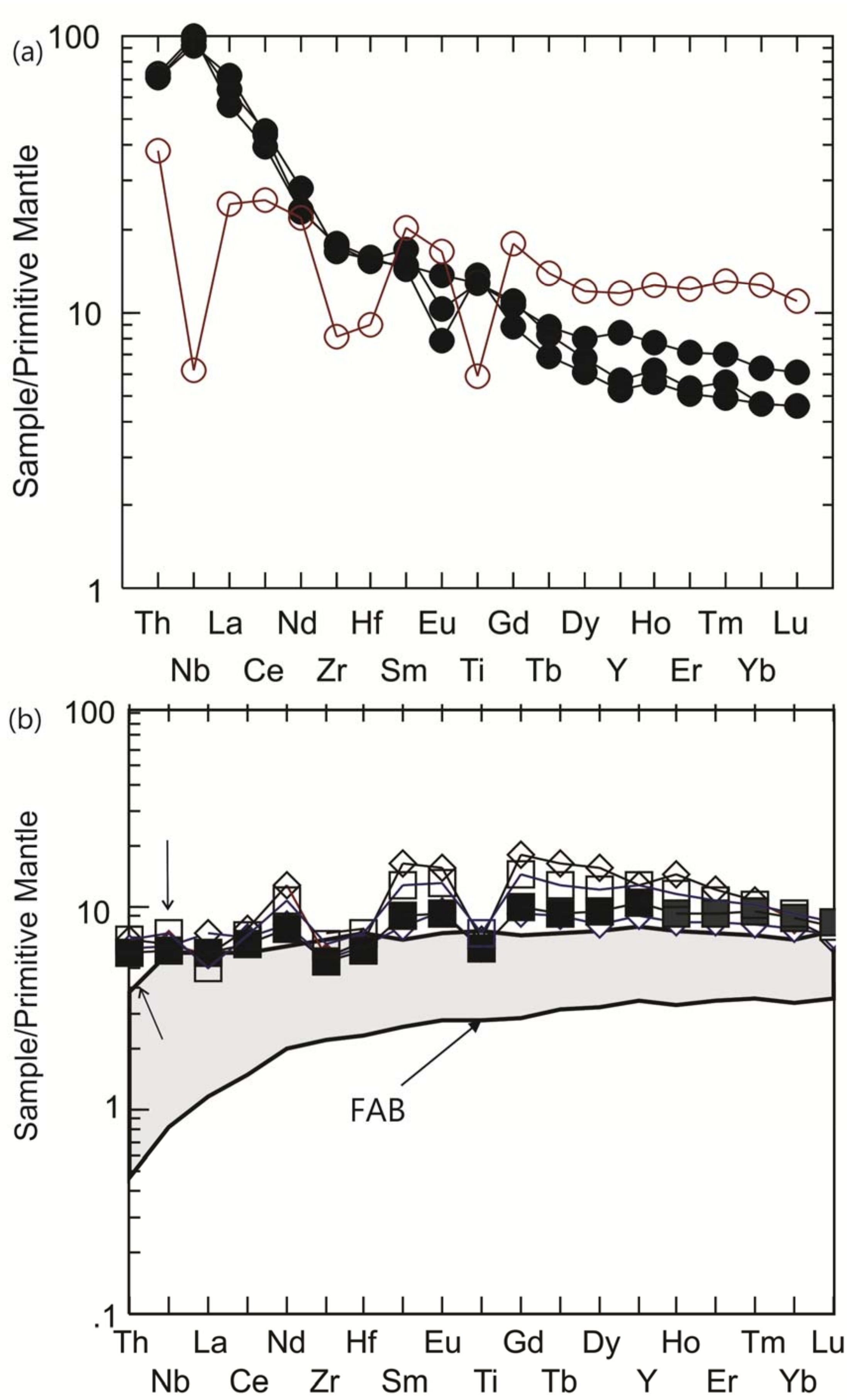
(a)
100
10
1
Sample/Primitive Mantle
Th
Nb
La
Ce
Nd
Zr
Hf
Sm
Eu
Ti
Gd
Tb
Dy
Y
Ho
Er
Tm
Yb
Lu
(b)
100
10
1
.1
Sample/Primitive Mantle
FAB
Th
Nb
La
Ce
Nd
Zr
Hf
Sm
Eu
Ti
Gd
Tb
Dy
Y
Ho
Er
Tm
Yb
Lu

Figure 10

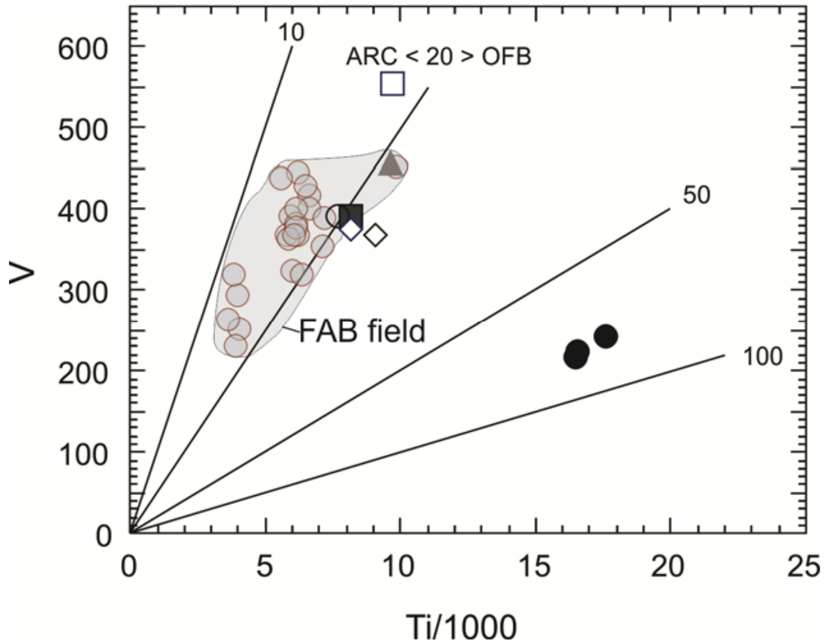

Figure 11.

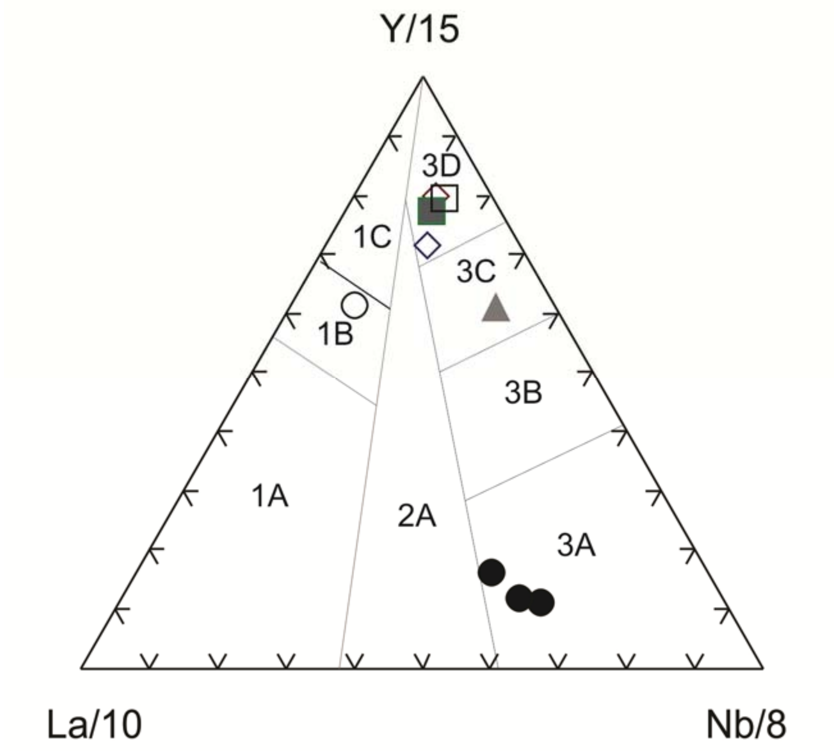

Figure 12.

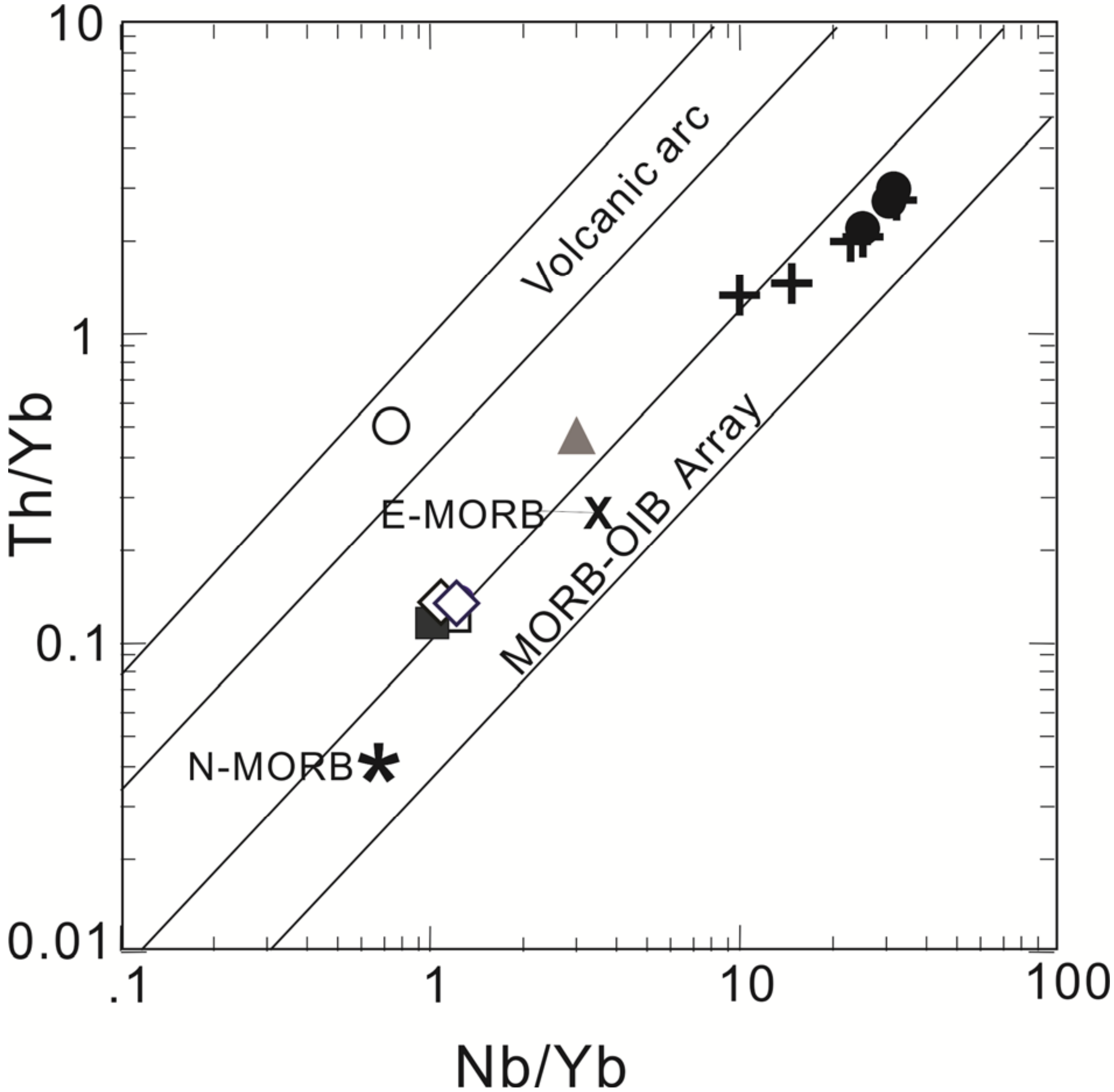
10
1
0.1
0.01
Th/Yb
.1
1
10
100
Nb/Yb
Volcanic arc
MORB-OIB Array
E-MORB
N-MORB

Figure 13.

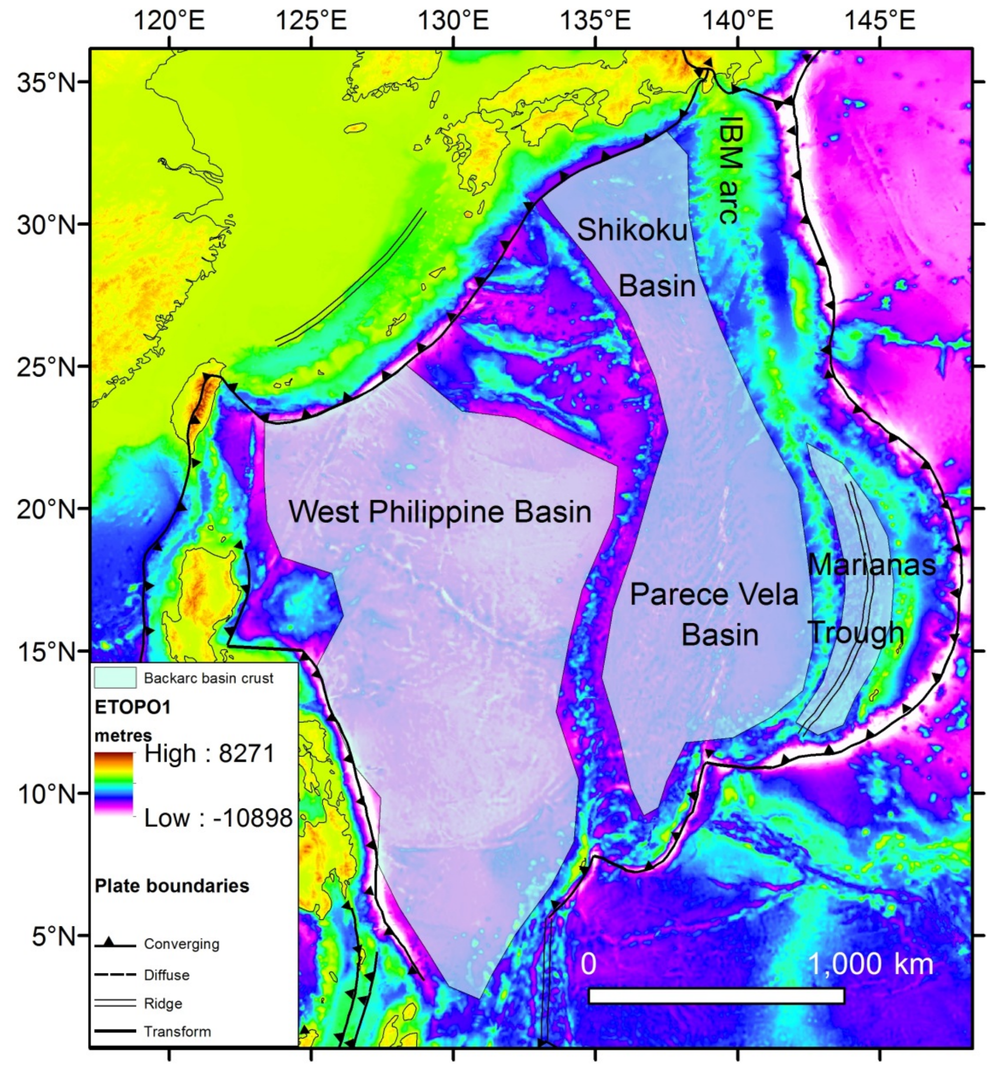
120°E
125°E
130°E
135°E
140°E
145°E
35°N
30°N
25°N
20°N
15°N
10°N
5°N
IBM arc
Shikoku
Basin
West Philippine Basin
Parece Vela
Basin
Marianas
Trough
0
1,000 km
Backarc basin crust
ETOPO1
metres
High : 8271
Low : -10898
Plate boundaries
Converging
Diffuse
Ridge
Transform

Figure 14.

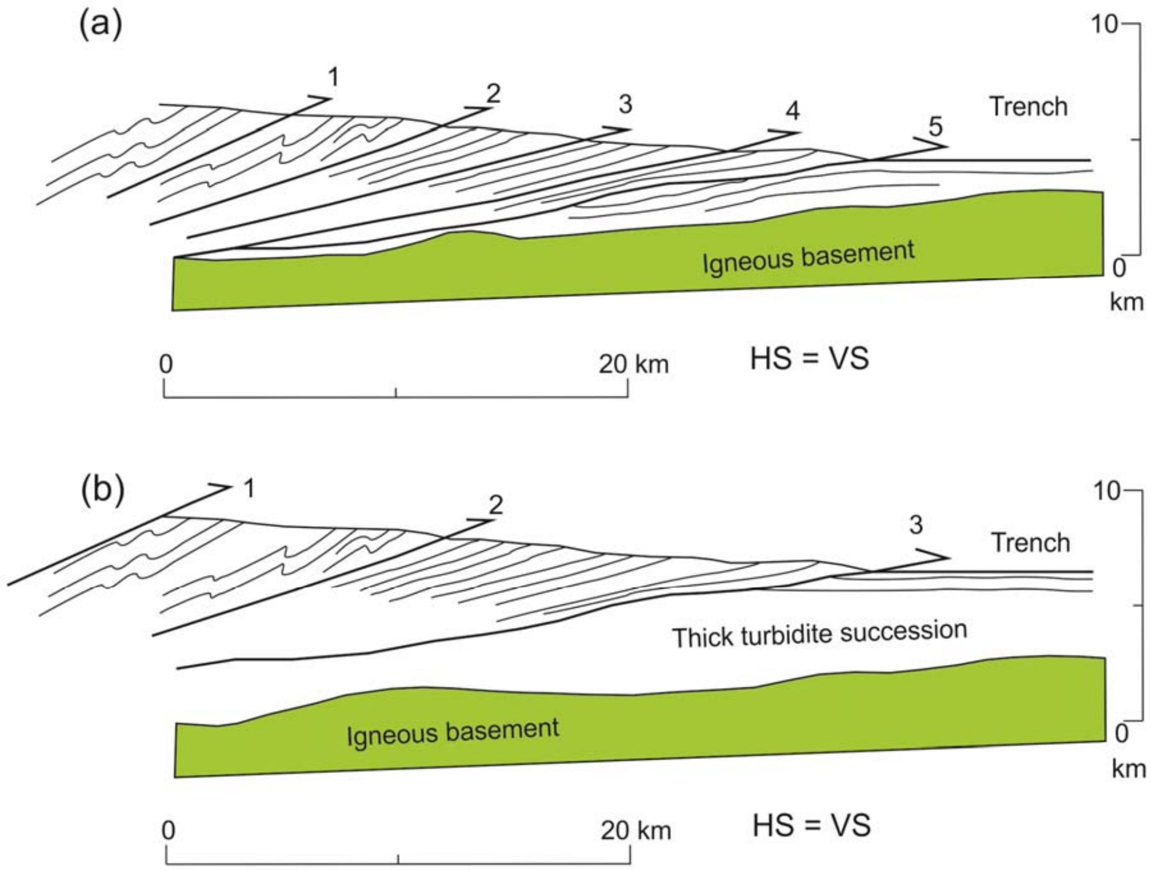
(a)
1
2
3
4
5
Trench
Igneous basement
10
0
km
0
20 km
HS = VS
(b)
1
2
3
Trench
Thick turbidite succession
Igneous basement
10
0
km
0
20 km
HS = VS

Figure 15.